Biogeosciences Discuss., 8, 9763–9811, 2011
www.biogeosciences-discuss.net/8/9763/2011/
doi:10.5194/bgd-8-9763-2011

Biogeosciences Discussions

Interaction between hydrocarbon seepage, chemosynthetic communities and bottom water redox at cold seeps of the Makran accretionary prism: insights from habitat-specific pore water sampling and modeling

D. Fischer[1], H. Sahling[1], K. Nöthen[2], G. Bohrmann[1], M. Zabel[1], and S. Kasten[1,2]

[1]MARUM – Center for Marine Environmental Sciences and Department of Geosciences, University of Bremen, Klagenfurter Strasse, 28334 Bremen, Germany
[2]Alfred Wegener Institute for Polar and Marine Research, Am Handelshafen 12, 27570 Bremerhaven, Germany

Received: 1 September 2011 – Accepted: 20 September 2011 – Published: 29 September 2011

Correspondence to: D. Fischer (dfischer@marum.de)

Published by Copernicus Publications on behalf of the European Geosciences Union.

Abstract

The interaction between fluid seepage, bottom water redox, and chemosynthetic communities was studied at cold seeps across one of the world's largest oxygen minimum zones (OMZ) located at the Makran convergent continental margin. Push cores were obtained from seeps within and at the lower boundary of the core-OMZ with a remotely operated vehicle. Extracted pore water was analyzed for sulfide and sulfate contents. Depending on oxygen availability, seeps were either colonized by microbial mats or by mats and macrofauna. The latter, including ampharetid polychaetes and vesicomyid clams, occurred in distinct benthic habitats which were arranged in a concentric fashion around gas orifices. At most sites colonized by microbial mats, hydrogen sulfide was exported into the bottom water. Where macrofauna was widely abundant, hydrogen sulfide was consumed within the sediment.

Numerical modeling of pore water profiles was performed in order to assess rates of fluid advection and bioirrigation. While the magnitude of upward fluid flow decreased from 11 cm yr^{-1} to <1 cm yr^{-1} and the sulfate/methane transition zone (SMTZ) deepened with increasing distance from the central gas orifice, the fluxes of sulfate into the SMTZ did not significantly differ (6.6–9.3 mol m^{-2} yr^{-1}). Depth-integrated rates of bioirrigation increased from 162 cm yr^{-1} in central habitats characterized by microbial mats and sparse macrofauna to 348 cm yr^{-1} in habitats of large and small vesicomyid clams. These results reveal that chemosynthetic macrofauna inhabiting the outer seep habitats at the lower boundary of the OMZ efficiently bioirrigate and thus transport sulfate into the upper 10 to 15 cm of the sediment. In this way bioirrigation compensates for the lower upward flux of methane in outer habitats and stimulates rates of anaerobic oxidation of methane (AOM) with sulfate high enough to provide sulfide for chemosynthesis. Through bioirrigation macrofauna engineer their geochemical environment and fuel upward sulfide flux via AOM. Due to the introduction of oxygenated bottom water into the sediment via bioirrigation the depth of the sulfide sink gradually deepens towards outer habitats. We therefore suggest that – in addition to the oxygen levels in

BGD
8, 9763–9811, 2011

the water column which determine whether macrofaunal communities can develop or not – it is rather the depth of the SMTZ and thus of sulfide production that determines which chemosynthetic communities are able to exploit the sulfide at depth. Moreover, large vesicomyid clams most efficiently expand the sulfate zone in the sediment and cut off smaller or immobile organisms from the sulfide source.

1 Introduction

Cold seep sites at the seafloor are created by the focused upward migration of both dissolved and/or gaseous hydrocarbons. Seeps are found at passive and active continental margins and generally show strong temporal and spatial variations in fluid flux (e.g. Wallmann et al., 1997, 2006; Suess et al., 1998; Tryon et al., 1999; Sahling et al., 2008; Niemann et al., 2009; Reitz et al., 2011). The upward supply of hydrocarbons towards and across the sediment/water interface produces steep geochemical gradients in the pore water and typically stimulates high rates of anaerobic oxidation of methane (AOM) and other hydrocarbons with sulfate close to the sediment surface (Borowski et al., 1996). The process of AOM which is performed by a consortium of archaea and sulfate-reducing bacteria (Hoehler et al., 1994; Hinrichs et al., 1999; Boetius et al., 2000) releases hydrogen sulfide and bicarbonate into the pore water at the so-called sulfate/methane transition zone (SMTZ). Hence, AOM fuels microbial and macrofaunal chemosynthetic life and generates a significant carbon sink through carbonate authigenesis (Ritger et al., 1987). Numerous studies have demonstrated that the flux of methane and sulfide towards the sediment/water interface determines the microbial and faunal community composition at cold seeps (e.g. Dando and Hovland, 1992; Barry et al., 1997; Sibuet and Olu, 1998; Sahling et al., 2002; Levin et al., 2003; van Dover et al., 2003; Arvidson et al., 2004; Levin, 2005; de Beer et al., 2006; Niemann et al., 2009; Lichtschlag et al., 2010a).

The convergent continental margin off Pakistan is referred to as the “Makran accretionary prism” after the Makran coastal desert. Cold seeps off Pakistan and their

BGD
8, 9763–9811, 2011

properties as habitats for chemosynthetic microbial and faunal life were described earlier (Faber et al., 1994; von Rad et al., 1996, 2000; Schmaljohann et al., 2001). Von Rad et al. (2000) found signs for gas seepage mostly on the upper slope (<1000 m) which they explained to result from local tectonic uplift and hence a destabilization of gas hydrates trapped within the gas hydrate stability zone at greater depth. These authors found that the occurrence of *Thioploca* sp. and/or *Beggiatoa* sp. mats in the area is confined to sites punctually expelling free gas or sites of drift-wood or other large pieces of organic matter on the sea floor (von Rad et al., 2000). It has been suggested that local variations in the spatial distribution of benthic, chemosynthetic macrofauna in the study area may be co-induced by the depth of AOM-derived sulfide supply and oxygen availability in the bottom water (von Rad et al., 1995, 1996, 2000; Schmaljohann et al., 2001).

The influence of bioirrigation and bioturbation on solute distribution and fluxes in marine sediments has been investigated in detail (e.g. Aller, 1980, 1984; Aller and Aller, 1998; Meile et al., 2001). However, only a few studies have quantified the influence of the activity of chemosynthetic biota on benthic fluxes at cold seeps (Wallmann et al., 1997; Haese, 2002; Haese et al., 2006). Bioirrigation, described as pumping of pore water by benthic fauna through their environment, is a prominent transport process at cold seeps as these sites are often densely colonized by chemosynthetic macrofauna. Wallmann et al. (1997) proposed that seep biota settling on and within the sulfidic seep sediments need to detoxify their habitats from high sulfide concentrations and do so by flushing their immediate surrounding with bottom water thereby introducing sulfate into the methanic zone of the sediment. On the other hand, macrofauna can only gain access to the sulfide pool needed for chemosymbiosis by digging down into the sediment. Besides sulfide removal by reaction with reactive (towards sulfide) iron phases (Berner, 1970), the distribution of sulfide within seep sediments and a potential sulfide export into the water column are controlled by both, the depths and rates of AOM as well as the activity of macrofauna colonizing the sediment surface. Due to the location of the "Makran" cold seeps within and below the core-OMZ and thus the

BGD
8, 9763–9811, 2011

distinct distribution of oxygen-dependent, bioirrigating/bioturbating (macrofauna) and anaerobic, non-irrigating (microbial mats) seep communities on the sediment surface the study area is ideal for exploring the interaction of water column redox, rates of upward fluid/gas migration, and bioirrigation in cold seep habitats.

In this study we investigate and quantify transport processes in different benthic seep-habitats of the Makran accretionary prism. The particular aim of this work is to elucidate the interaction between the intensity of fluid flux, oxygen levels in the bottom water, colonization with chemosynthetic biota, and solute fluxes towards and across the sediment/water interface. For this purpose we have carried out a visual examination (high definition camera) and video-targeted sediment sampling of distinct seep habitats within and below the core-OMZ by means of a remotely operated vehicle (ROV). We quantify pore water flow caused by advection and bioirrigation by means of 1-D modeling of pore water profiles. We show how seep-dependent macrofauna inhabiting the sediment surface actively shape their geochemical environment and thus control solute fluxes within the sediment and across the sediment/water interface.

2 Geological setting and local oceanography

At the Makran subduction zone oceanic crust of the Arabian plate and the Omara micro-plate dips northward underneath the Eurasian plate to form the Makran accretionary prism (Fig. 1). The deformation front of the Makran prism is located south of the first accretionary ridge at about 3000 m water depth and strikes West to East, parallel to the coastline of Pakistan (Kukowski et al., 2000, 2001; Ding et al., 2010). Convergence rates range from 36.5–42 mm yr^{-1} (Kukowski et al., 2001). A sediment package of 5–7 km thickness accumulated on top of the oceanic crust which is subject to subduction since at least the Oligocene (Schlüter et al., 2002). Kukowski et al. (2001) pointed out that sediments above the décollement are being accreted by imbricate thrusting forming well defined coast-parallel accretionary ridges. This N-S cascade of accretionary ridges was mapped in 1997 (Kukowski et al., 2000) and a distinct bottom simulating

BGD
8, 9763–9811, 2011

seismic reflector indicative for the phase boundary between free gas below and solid gas hydrates above has been described for the area (Kaul et al., 2000; von Rad et al., 2000; Ding et al., 2010).

The water column off Pakistan is characterized by a pronounced OMZ with oxygen concentrations <2 µM between 100 m and 1000 m water depth (Wyrtki, 1973). The OMZ is, however, subject to temporal variations in its vertical extent (Wyrtki, 1973; Olson et al., 1993). The thickness of the OMZ off Pakistan is controlled by the combined effects of moderate to high rates of aerobic degradation of organic matter in the water column and a sluggish supply with warm and saline intermediate waters derived from marginal seas as e.g. the Red Sea and the Persian Gulf (Olson et al., 1993).

3 Materials and methods

Sampling took place in the inter-monsoonal period in November 2007 during R/V *Meteor* cruise M 74/3 (Bohrmann et al., 2008). The main instrument of the cruise was the ROV *Marum-Quest 4000*. It was deployed at sites of gas discharge into the water column as recorded by echosounder gas flare imaging. Discrete sampling of individual seep habitats as visually identified based on different chemosynthetic microbial and macrobenthic communities was performed by ROV-operated push cores (PCs). Sampling included both the central as well as the surrounding habitats. We strictly avoided taking PCs in the immediate vicinity (<5 cm) of gas orifices. Push cores were taken from the different habitats of two seep sites located within the core-OMZ (site GeoB 12320 at "Flare 1", 551 m water depth, and site GeoB 12353 at "Flare 15", 732 m water depth) and two seep sites found at the lower boundary of the core-OMZ (site GeoB 12315, 1025 m water depth, and site GeoB 12313, 1038 m water depth – both at "Flare 2"). In addition to the habitat-specific sampling of these four seep sites two sediment cores from background sites unaffected by hydrocarbon seepage were retrieved with a TV-guided Multiple Corer (TV-MUC). The exact locations and characteristics of all sampling sites including the dominant chemosynthetic benthic communities of the individual habitats are listed in Table 1.

BGD
8, 9763–9811, 2011

3.1 Water column characteristics

Gas flare imaging was conducted with the ship-mounted parametric echosounder system *Atlas Parasound* as described by Nikolovska et al. (2008). In this study the notation "Flare", as it has been adopted from onboard echosounder identification of potential sampling targets, will be used to specify a major locality. In that, a "Flare" usually comprises a seafloor area of several tens of square meters including sites where more than one actual gas bubble stream was detected in the water column and where hydrocarbon seepage appeared bundled on the sea floor. Water column oxygen concentrations, temperature and salinity were determined with a Seabird 911 + CTD equipped with an SBE 43 (Seabird Electronics) oxygen sensor and temperature and salinity probes. These data were used as input parameters for geochemical modeling and flux calculations.

3.2 Identification of organisms

The ROV *Marum-Quest 4000* was equipped with a 3 Mega-pixel photo camera and two video cameras, one of them in HD quality. Images of these three systems were used for visual interpretation of seep habitats (Fig. 2). A tentative differentiation between *Beggiatoa* spp.-dominated and *Marithioploca* spp.-dominated (formerly known as *Thioploca* spp.; cf. Salman et al., 2011) microbial mats was achieved by means of the ROV-cameras. Admitting that this approach is rather weak compared to molecular biological techniques it may be stated that mats of both genera often appear in different shapes and structures. *Marithioploca* spp. were reported to appear as lawn-like, white filaments of sufficient length of several cm to sway in turbulent bottom waters and in a mat-thickness of several cm (Fossing et al., 1995; Schulz et al., 1996; Schulz and Jørgensen, 2001; Teske and Nelson, 2006; Salman et al., 2011). *Beggiatoa* spp. mats in contrast were often described to appear as white and/or orange-colored thin skins on the sediment surface with a mat thickness of less than one cm (Nelson et al., 1986; Robinson et al., 2004; Teske and Nelson, 2006; Salman et al., 2011).

BGD
8, 9763–9811, 2011

Macrofauna (used here as the collective term for clams, polychaetes) specimens were obtained by an ROV-operated net or collected onboard from retrieved PCs and immediately stored in vials filled with 96 % ethanol. In the following the central habitat of a seep site is termed "Habitat 1" and all successively occurring concentrically arranged habitats are termed "Habitat 2" and "Habitat 3".

3.3 Pore water sampling and analyses

After arrival of the ROV and the TV-MUC on deck the sediment cores were immediately transferred into the cold room (4 °C) of the ship and pore water was extracted within one hour by means of rhizons (Seeberg-Elverfeld et al., 2005). The average pore size of the rhizons is 0.1 µm and sampling resolution was 1 cm for the PC and 1–2 cm for the TV-MUC cores, respectively. Data shown at zero depth in this study represent bottom water concentration. Pore water aliquots for sulfate determination were diluted 1:100 and stored at −20 °C until analysis. Sulfate concentrations were measured by ion chromatography (IC) with an Advanced Compact IC 861 (*Metrohm*). Subsamples for the analysis of total dissolved sulfide ($\Sigma H_2S = H_2S + HS^- + S^{2-}$) were fixed in a 5 % Zn-acetate solution, kept at 4 °C and measured photometrically according to the methylene-blue method after Cline (1969). The reproducibility the above methods was checked by analyzing replicates of standards. The accuracy of all measurements was within ±3 %.

3.4 Diffusive flux calculations

Diffusive fluxes of sulfate and sulfide were determined according to Fick's first law of diffusion according to Eq. (1):

$$J_{(\text{species})} = -\Phi \times D_{\text{sed}} \times \frac{\delta C}{\delta X} \quad (1)$$

where $J_{(\text{species})}$ is the diffusive flux of the dissolved species, Φ represents sediment porosity (estimated 0.85), D_{sed} is the sediment diffusion coefficient in $m^2\,a^{-1}$ which

BGD
8, 9763–9811, 2011

was calculated for ambient bottom water temperature as determined by the CTD temperature sensor and corrected for tortuosity (Boudreau, 1997), and $\delta C\,\delta X^{-1}$ is the concentration gradient of the dissolved species in mol m^{-3} m^{-1}. Concentration gradients of sulfide and sulfate were derived from measured pore water profiles obtained for the individual seep habitats. Sulfate fluxes at site GeoB 12313 (Flare 2) were calculated from concentration gradients generated by modeled profiles.

3.5 Geochemical modeling with "CoTReM"

Pore water profiles obtained for PCs taken from the three distinct successive habitats of seep site GeoB 12313 (Flare 2; 1038 m water depth) located at the lower boundary of the OMZ were modeled with the computer software CoTReM. The aim of this simulation was to assess rates of fluid advection and bioirrigation. Site GeoB 12313 was chosen for simulation runs because gas hydrates were found within 40–100 cm sediment depth in the area of Flare 2 (Bohrmann et al., 2008) and thus the lower boundary concentration of methane in equilibrium with gas hydrates (85 mM) could be estimated in the model following Tishchenko et al. (2005). This approach is consistent, for example, with estimates of in situ methane concentrations used for pore water modeling at gas hydrate-bearing cold seeps on Hydrate Ridge off Oregon, USA (Torres et al., 2002) and at the Hikurangi Margin off New Zealand (Dale et al., 2010). Moreover, the spatial resolution was highest at site GeoB 12313 with three PCs obtained from adjacent habitats.

CoTReM is a one dimensional numerical, non-steady-state transport and reaction model based on an operator splitting approach. The software has been described in great detail elsewhere (e.g. Adler et al., 2000, 2001; Wenzhöfer et al., 2001; Pfeifer et al., 2002). Notably, CoTReM has already been successfully applied to model transport processes and geochemical reactions in other seep systems, namely mud volcanoes of the Eastern Mediterranean, by Haese et al. (2003) (simulation of AOM and advection rates) and Haese et al. (2006) (simulation of advection and bioirrigation rates).

BGD
8, 9763–9811, 2011

A model sediment column of 50 cm was chosen which was subdivided into cells of 1 mm thickness. The results are only displayed for the upper 30 cm of the sediment approximately corresponding to the length of the investigated PCs. Porosity was assumed to decrease from 0.9 at the sediment surface to 0.8 at a depth of 50 cm (lower model boundary). The time step to fulfill numerical stability was set to 10^{-4} yr. Bioirrigation was accounted for by implementing non-local mixing coefficients in the range of published values (e.g. Haese et al., 2006) until best-fit to measured sulfate profiles. Sedimentation rate was ignored due to the simulation of very short time scales. Measured bottom water concentrations of the chemical species involved define the upper boundary conditions. For methane, and at site GeoB 12313-6 (Habitat 1 at Flare 2) also for sulfide, fixed concentrations were defined at the lower model boundary that created the gradients necessary to simulate the respective fluxes into the model area from below. The only chemical reaction considered in the simulations was AOM with sulfate. Pre-defined maximum rates for AOM (0.5 mol dm^{-3} yr^{-1}) were used by the model as long as the educt species were available in sufficient amounts to create a narrow SMTZ. As soon as the concentrations decreased, the rates were automatically reduced to match the available amount of reactants in each cell in order to avoid negative concentrations. A compilation of input parameters for the simulation runs is given in Table 2.

In a second modeling approach we explored how an initially diffusion-dominated sediment/pore water system responds to upward advection and/or bioirrigation at different rates (see Sect. 5.4). The main question behind this simulation was to elucidate to which extent advective pore water flow – either through upward advection, or downward bioirrigation, or a combination of both – affects the depth of the SMTZ and fluxes of sulfate into the SMTZ. Boundary conditions chosen for the different scenarios were as described above, however in this approach we implemented the different transport processes consecutively in independent “scenarios”.

BGD
8, 9763–9811, 2011

4 Results

4.1 Background sites

Sulfate concentration profiles were obtained for two sites (TV-MUC cores GeoB 12309-3 and GeoB 12312-3) that were unaffected by gas release and did not show a colonization by chemosynthetic communities at the sediment surface. The sulfate profiles were linear at both sites and concentrations only slightly decreased with depth from bottom water values of 31 mM to about 29 mM at a depth of 20 cm in core GeoB 12309-3 and 26 mM at a depth of 23 cm in core GeoB 12312-3 (Fig. 3).

4.2 Gas seepage

At all four seep sites investigated in this study gas bubble ebullition from distinct gas orifices in the center of the seeps was observed. The gas orifices were about 1 cm in diameter. At the time of sampling gas flux at the shallower sites Flare 1 and Flare 15 (551 m and 732 m water depth) was generally lower than at Flare 2 (1025 m and 1038 m water depth; M. Römer, unpublished data). At the latter, which was located well within the GHSZ, gas bubbles emanating from the sea floor were immediately surrounded by skins of gas hydrate (M. Römer, unpublished data).

4.3 Seeps within the core-OMZ

The two seep sites GeoB 12320 (Flare 1, 551 m water depth; Fig. 2a) and GeoB 12353 (Flare 15, 732 m water depth; Fig. 2b) were located within the core-OMZ (oxygen concentrations <1 µM; Bohrmann et al., 2008) and above the GHSZ. Seep communities at both sites exclusively consisted of orange-colored microbial mats in the center (Habitat 1) surrounded by white/rose-colored microbial mats (Habitat 2; Fig. 2a and b). The overall diameter of these microbial mats was about 40 cm at Flare 1 (GeoB 12320) and about 60 cm at Flare 15 (GeoB 12353). Microbial mats at both sites were up to 1 cm thick and appeared chaotic and interwoven (Fig. 2a and b). Microbial mat coverage of

BGD
8, 9763–9811, 2011

the sediment surface was heterogeneous and single filaments could not be resolved with the HD camera. We tentatively identified the orange and white colored microbial mats at Flare 1 and 15 as *Beggiatoa* spp. or close relatives. Gas bubble emanation occurred from three distinct orifices within the orange mat at Flare 1 and from two orifices within the orange mat at Flare 15. Central, orange mats were always associated with dark-gray to black surface sediments (Fig. 2a and b) and we could observe blackish sediment grains entrained by gas bubbles ascending from the orifices. Bubble escape from the surrounding white/rose-colored mats was not observed. Authigenic carbonates of a very porous and brittle fashion were found in the surface sediments at Flare 1 and Flare 15. They exclusively occurred below microbial mats at gas vents.

Pore water data obtained for the central habitats at Flares 1 and 15 (GeoB 12320-9 and GeoB 12353-5, respectively; "Habitat 1" in Fig. 2a and b) show that sulfate concentrations were already well below sea water values close to the sediment surface (6.77 mM in core GeoB 12320-9 and 11.85 mM in core GeoB 12353-5) and further decreased with depth to minimum concentrations of 0.16 mM in GeoB 12320-9 and 0.92 mM in GeoB 12353-5 (Figs. 4a and 5a). Sulfide contents in the seep centers (Habitat 1) were relatively constant over depth and fluctuated between 5 and 6 mM, respectively (Figs. 4a and 5a). A concentration gradient of sulfide into the overlying bottom water was observed at both sites.

Sulfate profiles determined for the surrounding Habitats 2 at Flares 1 and 15 (GeoB 12320-4 and GeoB 12353-3 in Figs. 4b and 5b) show a steep, almost linear downward decrease from seawater values at the sediment surface to lowest concentrations fluctuating around 5 mM at 19 cm and 15 cm, respectively. Sulfide concentrations in both cores increase with depth along steep gradients to maximum values of 9.6 mM at 11 cm (GeoB 12320-4) and 10.7 mM at 13 cm (GeoB 12353-3). In these surrounding Habitats 2 of Flares 1 and 15 a sulfide concentration gradient into the bottom water was not observed.

BGD
8, 9763–9811, 2011

4.4 Seeps at the lower boundary of the OMZ

The two seep locations situated at the lower boundary of the core-OMZ at Flare 2 (site GeoB 12315 at 1025 m and site GeoB 12313 at 1038 m water depth; Fig. 2c and d) were characterized by slightly elevated bottom-water oxygen concentrations (>1 µM; Bohrmann et al., 2008) and abundant macrofaunal life both in the water column and at the sea floor. The sediment surface within both central habitats at Flare 2 was draped with m^2-sized patches of white/rose-colored microbial mats surrounding sites of active gas ebullition (Fig. 2c and d). The microbial mats (Habitat 1) at Flare 2 were about 1 m (GeoB 12313) and 5 m (GeoB 12315) in diameter, in places more than 5 cm thick and appeared as a lawn-like cover on the sediment surface. The mats at both central habitats at Flare 2 occurred around dm-sized cracks and fissures in the sediment. We could resolve single microbial filaments by means of the HD camera (Fig. 2e and f). However, filament diameter could not be estimated based on these photographs. At site GeoB 12315 we found the central microbial mats in Habitat 1 to be accompanied with and underlain by a cm^2-sized mat of orange-colored microbial filaments that showed a distinctly different appearance with a smaller mat thickness of about 1 cm (Fig. 2e). Due to the distinctly different filament lengths and pigmentation of both observed mat types we tentatively suggest that they belong to different species. The central small mat at site GeoB 12315 resembles *Beggiatoa* spp.-type filaments or close relatives (Fig. 2e) whereas the thick and vast white mats occurring at site GeoB 12313 and GeoB 12315 resemble *Marithioploca* spp. or close relatives (Fig. 2e and f).

The central microbial mats at Flare 2 were always surrounded by concentrically arranged habitats of chemosynthetic or grazing/filtering macrofauna (Habitats 2 and 3). The transition from Habitat 1 to Habitat 2 at the Flare 2 sites was marked by the co-occurrence of microbial mats associated with few small vesicomyid clams (cf. *Isorropodon* sp.) and abundant ampharetid polychaetes (Fig. 2f). Habitat 2 at both Flare 2 sites was generally dominated by the ampharetid polychaete *Pavelius uschakovi* (Kuznetsov and Levenshtein, 1988) and small (<3 cm) vesicomyid clams

BGD
8, 9763–9811, 2011

both decreasing in abundance in outward direction. The outermost Habitat 3 at both Flare 2 sites was dominated by small (<3 cm) and in places by larger vesicomyid clams. In contrast to the seep sites at Flares 1 and 15 (core-OMZ) a ubiquitous feature at both Flare 2 sites was the occurrence of massive authigenic carbonates that were up to a few dm in diameter. The carbonates were often but not exclusively found close to the gas orifices associated with microbial mats.

Pore water data were obtained for two PCs from seep site GeoB 12315 (Fig. 7) and for three PCs from seep site GeoB 12313 (Fig. 6). PC sampling of the central Habitat 1 sediments (GeoB 12315-9 and GeoB 12313-6) was partly complicated by the presence of massive authigenic carbonates. Sulfate concentration profiles obtained for these cores indicated that sulfate contents in the bottom water were depleted compared to bottom water at the background sites depicted in Fig. 3 and only showed a slight decrease down to a depth of about 5 cm (Figs. 6a and 7a). Below this depth sulfate concentrations sharply decreased to 8 mM (GeoB 12315-9) at 11 cm and 5 mM (GeoB 12313-6) at 10 cm sediment depth. In the central Habitat 1 of site GeoB 12313 sulfate concentrations increased again below 10 cm to reach values of 15 mM between 13 and 17 cm and then decreased downcore to reach values of about 2 mM at the base of the PC (Fig. 7a). Sulfide concentrations for the two Habitat 1 cores showed a steep downward increase from 1.5 mM at 1 cm depth to 16.5 mM at 13 cm depth (GeoB 12315-9, Fig. 6a) and from 4 mM at the surface to 17.5 mM at a depth of 10 cm (GeoB 12313-6, Fig. 7a).

Sulfate profiles of the Habitat 2 PCs GeoB 12315-4 (Fig. 6b) and GeoB 12313-12 (Fig. 7b) showed background concentrations at the sediment surface and a slight downward decrease within the first 6 and 10 cm, respectively. Below these depths, sulfate concentrations steeply dropped to 3 mM at a depth of 16 cm (GeoB 12315-4) and to 5 mM at a depth of 15 cm (GeoB 12313-12). Sulfide concentrations in both cores fluctuated between 0–2 mM in the upper 5–10 cm and increased along steep gradients to maximum values of 14 mM (GeoB 12315-4) and 8.5 mM (GeoB 12313-12) at 11 cm and 13 cm, respectively (Figs. 6b and 7b).

BGD
8, 9763–9811, 2011

In core GeoB 12313-13 obtained from Habitat 3 rather constant sulfate concentrations were measured from the sediment surface down to a depth of 15 cm below which sulfide showed a maximum of 6.4 mM at 19 cm and decreased downwards (Fig. 6c). In general, the depth of the distinct kink in the sulfate pore water profiles at both Flare 2 sites deepened with increasing distance to Habitat 1.

5 Discussion

5.1 Sulfate profiles and the depth of the SMTZ

Although displaying different profile shapes the interstitial sulfate concentrations at all investigated seep habitats decrease with depth indicating that AOM occurs close to the sediment surface. In contrast, sulfate contents at the two background sites GeoB 12309 and GeoB 12312 (Fig. 3) barely decrease over the sampled sediment interval and represent the "normal" pore water situation in the area which is governed by diffusion and neither affected by hydrocarbon seepage nor shallow AOM. The bottom water concentration of sulfate measured in the study area amounts to 31 mM (Fig. 3) and is thus slightly higher than average seawater sulfate values of ~28 mM (Claypool and Kaplan, 1974). Similarly high bottom-water sulfate concentrations were also reported by Schmaljohann et al. (2001) for sediment cores retrieved from comparable water depths on the Makran accretionary prism. A reasonable explanation for the elevated bottom water sulfate concentrations in the study area is the inflow of more saline intermediate water masses from marginal seas as e.g. the Red Sea and the Persian Gulf as has been proposed by Olson et al. (1993).

Sulfate profiles obtained for the core-OMZ sites (Flares 1 and 15, Figs. 4 and 5) depict distinctly different shapes compared to those obtained for the lower OMZ-boundary locations (Flare 2, Figs. 6 and 7). At the core-OMZ sites we found sulfate contents well below measured ambient bottom water values (~31 mM) at the sediment surface in the central habitats colonized by orange microbial mats (GeoB 12320-9, GeoB 12353-5).

BGD
8, 9763–9811, 2011

Following the interpretation by Niemann et al. (2006), the low sulfate concentrations at the sediment surface in the central habitats may be caused by fluid advection inhibiting the diffusion of sulfate into the sediment. Advection usually produces a concave-down curved sulfate profile which was found to a minor extent at the core-OMZ site GeoB 12353-5 (Fig. 5a). For the outer habitats ("Habitat 2") of Flares 1 and 15, which were colonized by white microbial mats, we determined linear sulfate profiles that suggest a diffusion-controlled depth of the SMTZ (Figs. 4b and 5b).

In contrast to the core-OMZ sites, sulfate profiles obtained for all habitats at Flare 2 located at the lower boundary of the OMZ uniformly show distinct "kink-type" or "irrigation-type" profiles (Aller, 1980; Aller and Aller, 1998; Hensen et al., 2003) several cm below the sediment surface (Figs. 6 and 7). Kink-type sulfate profiles suggest intense irrigation of the sediment surface with sulfate-rich bottom water by polychaetes and clams colonizing these habitats (e.g. Fossing et al., 2000; Haese et al., 2006). Yet, based on the limited bottom water oxygenation at Flare 2, we suggest the polychaete and clam communities can only be sustained if the OMZ in the water column either shrinks or shifts periodically and in that way provides enough oxygen for these communities. In fact, it has been stated earlier that the vertical extent of the OMZ off Makran is not stable and undergoes monsoon-forced fluctuations (Wyrtki, 1973; Brand and Griffiths, 2009). It is thus likely that Flare 2 is periodically flushed with oxygen-rich bottom water sustaining the observed macrofauna. The strong depletion in sulfate observed at a depth of several cm in all Habitat 1 cores indicates that the SMTZ was recovered in the sampled sediment intervals and is usually located between 5 and 15 cm (Figs. 4a, 5a, 6a and 7a). At all Habitat 2 and 3 sites the approximate depth of the SMTZ is located slightly deeper between 10 and 20 cm (Figs. 4b, 5b, 6b, 7b and 7c). At site GeoB 12313, where three PCs were retrieved, we found that the depth of the SMTZ progressively deepens from the center towards the outer habitats (Fig. 7).

It is difficult to identify the exact depths of the SMTZ at the four investigated seep sites because sulfate concentrations in all habitats except for site GeoB 12313-6 approach relatively constant concentrations around a few millimoles below the assumed depth of

BGD
8, 9763–9811, 2011

the SMTZ and do not completely vanish in the reaction zone. Some possible scenarios were suggested to explain similar observations at other seeps, including mixing of bottom water into the sediment due to ex situ degassing based on pressure release (Wallace et al., 2000) or ebullition of free gas in situ (Haeckel et al., 2007). Particularly the latter process needs to be considered in all Habitat 1 sites where bubble escape was observed. Oxidation of sulfide to sulfate during sample handling and storage has been discussed in several studies (Luff and Wallmann, 2003; Leloup et al., 2007) but may be of minor significance here due to immediate dilution and freezing of sulfate samples onboard ship. "Cryptic sulfur cycling" based on disproportionation of intermediate sulfur species releasing sulfate within the methane zone was identified by Holmkvist et al. (2011) to explain low sulfate contents in sediments of the Black Sea. We cannot exclude this process; however, sulfate concentrations reported here are much higher than those shown by Holmkvist and co-workers. Threshold sulfate concentrations up to 2 mM constraining bioenergetics for bacterial sulfate reduction (Leloup et al., 2007; Knab et al., 2008) and AOM (Dale et al., 2010) were suggested to explain sulfate tailing below the SMTZ which may be of significance at sites GeoB 12315-4 and GeoB 12353-5 where we measured near-constant sulfate levels around 2 mM below the SMTZ. For sites close to in situ gas bubble ebullition (Habitats 1 in this study) a lateral flow of sulfate-rich pore water towards the gas bubble conduit involving convection-like pore water cycling was proposed which would lead to sulfate transport into a discrete layer below the SMTZ (O'Hara et al., 1995; Tryon et al., 2002; Haeckel and Wallmann, 2008). It was shown in detail by O'Hara et al. (1995) that a draw-down of bottom water into the sediment occurs at gas seeps off Denmark within a lateral distance of up to 20 cm from the gas orifice. Habitat 1 core GeoB 12313-6 provides strong evidence for this kind of convective flow because the sulfate profile displays a peak between 10 and 20 cm pointing at a source of sulfate to the pore water in this depth interval (Fig. 7a). The core was obtained within a distance of <30 cm from the gas orifice (Fig. 2d) and could thus be affected by convection of bottom water through the sediment (O'Hara et al., 1995). Habitats 2 and 3 cores at Flare 2, however, were obtained from sites several m

BGD
8, 9763–9811, 2011

away from the orifice (Fig. 2d) and may thus not be influenced by a draw-down of bottom water into the sediment which is supported by the absence of pronounced sulfate peaks below the SMTZ (Fig. 7b and c). In contrast, Habitat 2 cores at Flares 1 and 15 (Fig. 2a and b) were retrieved within a radius of only 20 cm around the respective gas orifices and indeed show minor increases in sulfate contents at 12 cm (GeoB 12320-4) and 17 cm (12353-3) which suggest lateral flow of sulfate-rich bottom water into the sediment (Figs. 4b and 5b). Our interpretation of convection-like cycling of pore and bottom water is in accord with the study by O'Hara et al. (1995) stating that convective cycling of pore and bottom water at gas seeps is an important transport mechanism at sites close to the gas orifice and may influence rates of biogeochemical turnover of dissolved species as e.g. sulfate.

5.2 Hydrogen sulfide fluxes and chemosynthetic communities

Concentration gradients used for flux calculations are indicated as black lines in Figs. 4, 5, 6 and 7. Upward sulfide fluxes were calculated for the Habitat 2 sites at Flare 1 and Flare 15 (GeoB 12320-4 and GeoB 12353-3) which were not affected by gas bubble escape at the time of sampling. An export of sulfide into the bottom water is not indicated by pore water profiles at both sites (Figs. 4b and 5b). The sulfide flux at these sites amounts to 4.9 and 3.3 $mol\,m^{-2}\,yr^{-1}$, respectively, and is directed towards the sediment surface where white microbial mats were observed (Table 3). The calculated sulfide flux is in the lower range of published values for comparable microbial mat habitats for example at the Cascadia margin (Sahling et al., 2002) and at the Håkon Mosby Mud Volcano (de Beer et al., 2006; Lichtschlag et al., 2010a). In fact, Lichtschlag et al. (2010a) found that a sulfide flux of 2.5 $mol\,m^{-2}\,yr^{-1}$ represents the lower threshold for *Beggiatoa* mats which is well below the fluxes calculated for the Habitat 2 cores at Flares 1 and 15. In agreement with Gilhooly et al. (2007) we found at the core-OMZ sites that orange microbial mats (Habitat 1) seem to tolerate high sulfide concentrations and fluxes towards and across the sediment/water interface, whereas white microbial mats (Habitat 2) tolerate only moderate to low sulfide concentrations.

BGD
8, 9763–9811, 2011

At the microbial mat site GeoB 12313-6 (Habitat 1, Flare 2, lower boundary of OMZ) a sulfide flux across the sediment/water interface is indicated by the sulfide profile (Fig. 6a, inset). The sulfide export into the bottom water amounts to 1.3 mol m^{-2} yr^{-1}. We have observed numerous microbial filaments that were attached to carbonate chunks or polychaete tubes exposed above the sediment surface and that were thus cut off from the interstitial sulfide pool in the sediment (Fig. 2f). Apparently, the sulfide flux across the sediment/water interface is sufficient to nourish these microbes at site GeoB 12313-6 and probably at the comparable Habitat 1 site GeoB 12315-9 (Flare 2). A similar observation has been reported from cold seeps on the Hikurangi Margin (Sommer et al., 2010) which indicates that thiotrophic microbes do not necessarily depend on direct access to the pore water sulfide pool as long as the sulfide export into the bottom water meets their sulfide demand.

Apart from the sulfide flux across the sediment/water interface in Habitat 1 at site GeoB 12313 we determined the "deep" upward sulfide flux from the SMTZ to depths of 5 to 15 cm at all Flare 2 sites. In general we found that the "deep" sulfide flux amounts to 8.0 and 9.2 mol m^{-2} yr^{-1} at the microbial mat sites (Habitat 1, GeoB 12313-6 and GeoB 12315-9) while fluxes of 5.7 and 11.0 mol m^{-2} yr^{-1} were determined for the polychaete and clam sites GeoB 12313-12 and GeoB 12315-4 (Habitat 2). The lowest flux of 3.9 mol m^{-2} yr^{-1} was obtained for the large clam site GeoB 12313-13 in Habitat 3 (Table 3). Despite the rather high flux at site GeoB 12315-4 (Habitat 1), the sulfide flux in general decreases slightly towards outer habitats at Flare 2. This pattern resembles findings by Sahling et al. (2002) who calculated a high sulfide flux of 23 mol m^{-2} yr^{-1} below a *Beggiatoa* mat and a lower flux of 6.6 mol m^{-2} yr^{-1} below a clam bed (large *Calyptogena*) at Hydrate Ridge cold seeps.

Upward sulfide fluxes have been widely used in recent publications to describe the geochemical environment of chemosynthetic communities at cold seeps (e.g. Sahling et al., 2002; de Beer et al., 2006; Niemann et al., 2009; Lichtschlag et al., 2010b). It needs to be stressed that the sulfide profiles measured in sediments inhabited by chemosynthetic organisms are already influenced by the metazoan sulfide uptake and

BGD
8, 9763–9811, 2011

thus calculated fluxes may be a result rather than a prerequisite for chemosynthesis. In Table 3 we show the depth intervals of the steepest sulfide gradients for the three cores at site GeoB 12313. The depths gradually increase towards the outer habitats from 3–7 cm near the gas orifice (GeoB 12313-6) to 15–18 cm in the outermost Habitat 3 (GeoB 12313-13) where abundant large and small vesicomyid clams were observed. The clams, although depending on a certain sulfide flux for their symbionts (e.g. Grehan and Juniper, 1996; Sahling et al., 2005), ventilate sulfide-free bottom water into the sediment and at the same time remove sulfide from the pore water for respiration. Our data show that the magnitude of the upward sulfide flux alone does not determine the colonization of the sediment by chemosynthetic organisms exploiting the sulfide pool and does thus not accurately describe their geochemical environment. It is rather the combination of sulfide flux, the depth of sulfide release (SMTZ) and the depth into which the flux occurs, i.e. the depth where sulfide is depleted either due to mineral authigenesis or uptake by organisms which determines the colonization of seeps by thiotrophic and/or chemosynthetic communities.

5.3 Quantifying transport processes – modeling results

The computer model CoTReM has been applied to the three habitats of site GeoB 12313 at Flare 2 below the core-OMZ. 3-D-modeling of pore water profiles considering the seep including all habitats as a continuum would be favorable at the study site Flare 2. However, such an approach would require a much higher sampling density than was achieved during the cruise. For example, the pore water profiles used for modeling derive from three PCs obtained from distinctly different habitats at Flare 2 selected by eye. The investigated habitats in total covered an area of more than 25 m^2 which is estimated based on observed colonization with chemosynthetic communities. Thus, the pore water profiles of a single PC would represent an area of more than 8 m^2 which is not sufficient for 3-D-modeling. We therefore considered each PC to be representative for its respective habitat and applied the 1-D-model in order to estimate the magnitude pore water transport processes. Simulated profiles of sulfate and sulfide at

BGD
8, 9763–9811, 2011

site GeoB 12313 are depicted as solid lines in Fig. 6 and advection and bioirrigation rates are given in Table 4.

Advective flow velocity is highest (11 cm yr^{-1}) in core GeoB 12313-6 in the vicinity of the gas orifice and decreases with increasing distance to the orifice in cores GeoB 12313-12 (8 cm yr^{-1}) and GeoB 12313-13 (<1 cm yr^{-1}). Few published pore water flow velocities of 10 cm yr^{-1} (Linke et al., 2005), 3–50 cm yr^{-1} (Haese et al., 2003, 2006) and 1–28 cm yr^{-1} (Han and Suess, 1989) determined for cold seeps on the Cascadia margin and mud volcanoes on the Costa Rica margin and in the Mediterranean Sea compare well to the rates determined here. Yet, the majority of studies depicts much higher velocities of up to several meters yr^{-1} (e.g. Linke et al., 1994; Wallmann et al., 1997; Lichtschlag et al., 2010b). The low advection rates determined here may be due to the fact that cold seeps that are not associated with mud volcanism emit fluids and gas rather continuously and fluid flow is generally slow. In contrast, mud volcanoes, expel mixtures of gas, fluid and mud at high velocities during eruptive phases (cf. Kopf, 2002).

Depth-integrated rates of bioirrigation increase from 120 cm yr^{-1} in Habitat 1 to 210 cm yr^{-1} in Habitat 2 and 297 cm yr^{-1} in Habitat 3 including nonlocal mixing coefficients of 100–120 yr^{-1} (Table 4). The rates correspond exceptionally well with those obtained for a Mediterranean mud volcano by Haese et al. (2006) with a similar approach using CoTReM. Depth-integrated bioirrigation rates of up to 900 cm yr^{-1} were obtained by Wallmann et al. (1997) to simulate bioirrigation at active cold seeps in the Aleutian subduction zone. The higher values used by these authors are probably linked to the fact that the pore water advection obtained by Wallmann et al. (1997) is with 340 cm yr^{-1} much higher than the maximum velocity determined in this study (11 cm yr^{-1}). Therefore, organisms responsible for bioirrigation at the Aleutian margin seeps had to counteract a much higher advective flow velocity in order to detoxify their habitat from too high sulfide concentrations.

The pore water model produces considerably higher maximum concentrations of hydrogen sulfide than those measured in cores GeoB 12313-12 and GeoB 12313-13

BGD
8, 9763–9811, 2011

(Fig. 6). The deviation of modeled maximum sulfide concentrations compared to measured values is attributed to the fact that the model in our configuration neglects the various processes of sulfide consumption e.g. sulfide uptake by organisms (e.g. Arp et al., 1984), precipitation of iron sulfides (e.g. Berner, 1970) or sulfurization of organic matter (e.g. Brüchert, 1998). Regarding the formation of iron sulfide minerals, the availability of reactive Fe(III) species may play an important role: the Habitat 1 site GeoB 12313-6 is interpreted to be subject to most intense and shallowest production of sulfide via AOM due to highest rates of advective transport of methane-rich fluids. In theory, prolonged production of sulfide through AOM would result in a continuous reduction and removal of reactive iron (oxyhydr)oxides via reaction with hydrogen sulfide until most of the Fe(III) minerals are transformed into iron monosulfides and pyrite (Berner, 1970). Consequently, sites GeoB 12313-12 and GeoB 12313-13, which are subject to lower rates of AOM and sulfide release than the central site GeoB 12313-6, may have experienced a less intense reduction of iron (oxyhydr)oxides. Thus, due to the fact that the only chemical reaction we used in CoTReM is AOM, one would expect that the overestimation of hydrogen sulfide concentrations by the model would be greater in distant sites (Habitats 2–3) than in the central one (Habitat 1) which is well supported by our data (Fig. 6).

5.4 Schematic evolution of the depth of the SMTZ and sulfate fluxes – unraveling the relative importance of different transport processes

The studies by Wallmann et al. (1997) and Haese et al. (2006) demonstrated that the interaction of the transport processes bioirrigation and advection significantly influences pore water profiles and solute fluxes at cold seeps. In this chapter we contribute further insights into the magnitude and importance of the complex interplay of up- and downward transport processes based on habitat-specific pore water modeling: Fig. 8 depicts a simulated stepwise development of the pore water profiles at site GeoB 12313 from a purely diffusion-controlled system towards the present measured state including upward advection and downward bioirrigation. The initial setting for the simulation includes molecular diffusion as the only transport process (Fig. 8, scenario A). It is

BGD
8, 9763–9811, 2011

obvious that the shapes of the sulfate profiles, sulfate fluxes and the depths of the SMTZ in Fig. 8, scenario A do not match the measured ones depicted in scenario D. Upward advection was thus simulated for the three habitats at different rates in order to approach the observed sulfate gradients (and fluxes) into and the depths of the SMTZ (Fig. 8, scenario B). We have discussed earlier that the pore water profiles at site GeoB 12313 are likely influenced by a convection-like pore water flow, where the central Habitat 1 experiences lateral inflow of bottom water balancing the focused gas escape (O'Hara et al., 1995). Although the model does not consider lateral advection, it was possible to simulate the sulfate concentration gradients and particularly the respective depths of the SMTZs in both cores of Habitat 2 and 3 with upward advection. We therefore suggest that an upward advective flow of pore water is present in all modeled habitats at Flare 2. The onset of advective pore water flow pushes the SMTZ towards the sediment surface in all cores and significantly increases sulfate fluxes into the SMTZ in all habitats (Fig. 8, scenario B). The upward-shifted SMTZ leads to a shallower sulfide release via AOM and thus triggers an increase in sulfide flux towards the sediment surface in all habitats. In Habitat 1 where the SMTZ is shallowest (Fig. 8, scenario B) the sulfide flux towards the sediment surface is highest and it decreases towards outer habitats because the sulfate fluxes into the reaction zone decrease in the same direction. Thus, the high advection of pore water in Habitat 1 triggers sulfide flux to the sediment surface that meets the high sulfide demand of microbial mats (de Beer et al., 2006). In contrast, the lower advection in Habitats 2 and 3 leads to a weaker upward sulfide flux that meets the demand of chemosynthetic macrofauna, for example clams and polychaetes (Sahling et al., 2005). We assume that scenario B in Fig. 8 represents the first step in seep colonization which determines whether the sediment surface is colonized by microbial mats in the center (highest sulfide flux) or by chemosynthetic macrofauna (lower sulfide flux in Habitats 2 and 3). Consequently, simulating the colonization of the seep with chemosynthetic organisms, non-local mixing coefficients (bioirrigation at different rates, Table 4) were implemented into the model to account for bioirrigation (Fig. 8, scenario D). Implementation of bioirrigation as a further

BGD
8, 9763–9811, 2011

transport process leads to the distinct gradient changes ("kink-type") that we observed in the measured sulfate profiles and at the same time shifts the SMTZ to greater depths due to introduction of sulfate-rich bottom water into the sediment (Fig. 8, scenario D). To test, if the depth of the SMTZ, sulfate fluxes, and shapes of the sulfate profiles can be sufficiently simulated considering only diffusion and bioirrigation without upward advection, we started a separate run (Fig. 8, scenario C). In this case the general sulfate profile shapes more or less match those of measured profiles, yet the depths of the SMTZ and sulfate fluxes do not, which highlights the importance of upward advection for the three examined sites.

The development of the sulfate fluxes in the different habitats and in the different model scenarios needs further consideration, because the sulfate input into the SMTZ determines the concentration and flux of released sulfide, which is essential for chemosynthetic communities. In Fig. 8 (scenario D, "present state") the sulfate fluxes into the SMTZ are given as bold numbers. The fluxes slightly decrease from 9.3 $\mathrm{mol\,m^{-2}\,yr^{-1}}$ in the center to 7.7 $\mathrm{mol\,m^{-2}\,yr^{-1}}$ and 6.6 $\mathrm{mol\,m^{-2}\,yr^{-1}}$ in the outer Habitats 2 and 3. When considering only advection (Fig. 8, scenario B) sulfate fluxes decrease stronger in the same direction, whereas sulfate fluxes stay similar when considering only bioirrigation (Fig. 8, scenario C). This shows that the combined transport processes advection and bioirrigation produce a mixed signal in the fluxes of sulfate into the SMTZ. Thus, the ventilating macrofauna counteract upward advection by shifting the SMTZ to greater depth but at the same time lead to comparably high sulfate fluxes (and high rates of sulfide production) in all three habitats.

The stepwise simulation in Fig. 8 shows that it is the combination of upward advection and counteracting downward transport of bottom water by chemosynthetic macrofauna that resulted in the best fit of the depth of the SMTZ, sulfate fluxes into the reaction zone and the general shapes of the sulfate profiles in all three habitats at Flare 2. Compared to earlier studies (e.g. Wallmann et al., 1997; Haese et al., 2006) targeted sampling of distinct seep-habitats enabled us to quantify the complex interplay of bioirrigation and advection and their impact on solute fluxes in the three different habitats at Flare 2.

BGD
8, 9763–9811, 2011

5.5 The mutual interaction of geochemistry and chemosynthetic communities

Comparing core-OMZ seeps (Flare 1 and 15) to those at the lower boundary of the OMZ (Flare 2) the most prominent feature is that oxygen levels in the bottom water determine whether a cold seep is colonized exclusively by microbial mats or by mats and surrounding chemosynthetic macrofauna including ampharetid polychaetes and vesicomyid clams. We could show that the macrofauna – most probably the observed clams – compensate for lower upward advection in outer habitats compared to the microbial mat habitat by shifting the SMTZ to greater depth which induces high sulfate fluxes and intense sulfide release. This is summarized in the conceptual model given in Fig. 9. This figure shows how animals ventilating the sediment surface with bottom water lead to an extended sulfate zone and thus provide oxic (or at least non-sulfidic) conditions (Fig. 9b). Seeps within the OMZ lack colonization by metazoans which allows a very shallow SMTZ to develop (Fig. 9a). The fact that clams shift the SMTZ to greater depth implies that they may gradually proceed towards the seep-center attracted by the shallow and high sulfide flux and may at the same time undermine and thus cut off smaller organisms (cf. Habitat 1–2 in this study) from the sulfide source (Figs. 8 and 9). In that way the clams progressively broaden the sulfate zone and thus eventually dominate the respective habitats. It is important to note that the irrigating activity of (large) clams does not only help to detoxify their own habitat from too high sulfide concentrations (Wallmann et al., 1997) but could be an opportunistic means in order to gain advantage over competitive, smaller organisms in accessing the sulfide pool in the sediment. Sommer et al. (2008, 2010) argued that ampharetid polychaete habitats at cold seeps (cf. Habitats 2 at Flare 2 in this study) may represent an early stage of seep-colonization by metazoans. Based on our findings we wish to expand upon this idea by suggesting that the occurrence of large clams in the vicinity of gas orifices and without "transient" habitats of medium-sized organisms such as polychaetes or smaller clams may indicate a mature stage of a cold seep-ecosystem, where polychaete and small clam communities have been undermined and cut off from the sulfide

BGD
8, 9763–9811, 2011

source in the sediment by the opportunistic and dominant large clams. This statement is further supported by the observation of cold seeps at greater depth (~1850 m) in the Makran area which are almost exclusively colonized by large (<10 cm) vesicomyid clams in the vicinity of gas orifices lacking any distinct microbial mat, polychaete or small clams habitats ("Flare 6", cf. Bohrmann et al., 2008). It is striking in this respect that these sites are additionally characterized by massive pavements of authigenic carbonates at the sea floor. In contrast to the deeper Flare 6 (cf. Bohrmann et al., 2008) sites within and at the lower boundary of the core-OMZ investigated in this study may represent rather young/juvenile seep ecosystems. This is suggested by vast "transient" habitats of small chemosynthetic clams and polychaetes (Flare 2) and the sparse occurrence of authigenic carbonates (Flares 1, 2 and 15).

6 Summary and conclusions

This is one of the first studies which examined the interplay of bioirrigation and advection in defined cold seep habitats across a marine oxygen minimum zone (OMZ). We performed targeted push core sampling with a remotely operated vehicle and conducted pore water analyses in different habitats at four seep-sites. Sites within the core-OMZ are characterized by linear sulfate profiles and the absence of metazoan life. Sites at the lower boundary of the OMZ depict pronounced kink-type sulfate profiles and are characterized by at least three distinct habitats arranged in a concentric fashion around the gas orifice that are dominated by microbial mats, ampharetid polychaetes, or vesicomyid clams. Pore water modeling was conducted for a seep at Flare 2 at the lower boundary of the OMZ. The simulation revealed that upward advection is highest near the gas orifice and decreases towards the outer habitats, whereas depth-integrated rates of bioirrigation increase in the same direction due to changes in the chemosynthetic communities. Hydrogen sulfide fluxes towards the sediment surface at all sites only slightly decrease towards outer habitats. A sulfide export into the bottom water was found in three of four central habitats colonized by microbial mats,

BGD
8, 9763–9811, 2011

whereas sulfide is depleted at or below the sediment surface in the other habitats. It appears that chemosynthetic macrofauna in outer habitats, here polychaetes and/or clams, compensate for lower supply with sulfide triggered by low advection rates, i.e. methane flux, by introducing oxygenated and sulfate-rich bottom water into the sediment. Furthermore, bioirrigation considerably shifts the SMTZ towards greater depths. At the same time steep gradients and comparably high fluxes of sulfate into the SMTZ are established in all three habitats which fuel hydrogen sulfide release via anaerobic oxidation of methane. We could thus show that chemosynthetic communities dominated by clams and polychaetes actively shape their geochemical environment by shifting the SMTZ towards depth and gain selective advantage over passive or immobile organisms (e.g. thiotrophic microbes) competing for sulfide in the sediment. Taking into account that macrofauna depend on oxygen supply we propose that it is the mutual influence of bottom water redox geochemistry and burrowing chemosynthetic organisms that determines the depth of the SMTZ at cold seeps.

Acknowledgements. We are indebted to the captain, crew and the shipboard scientific party of R/V *Meteor* cruise M 74/3 for excellent support and cooperation. André Gaßner and Karsten Enneking (University of Bremen) are thanked for laboratory assistance onboard ship as well as onshore. We would like to thank K. Zonneveld (University of Bremen) for conducting CTD casts and oxygen measurements during the cruise. H. N. Schulz-Vogt (MPI for Marine Microbiology, Bremen) greatly helped with the identification of seep-organisms. Matthias Haeckel (IFM-GEOMAR, Kiel), Jörn Peckmann (MARUM, Bremen; now University of Vienna), and Michael Schlüter (AWI, Bremerhaven) are thanked for numerous valuable discussions. Thanks to Dieter Fiege (Senckenberg Forschungsinstitut) for polychaete identification. REVIEWERS. This study was funded through the DFG-Research Center/ Cluster of Excellence "The Ocean in the Earth System" (MARUM). We acknowledge further financial support from the Helmholtz Association (AWI, Bremerhaven). All data are available on the database Pangaea (http://www.pangaea.de).

BGD
8, 9763–9811, 2011

References

Adler, M., Hensen, C., Kasten, S., and Schulz, H. D.: Computer simulation of deep sulfate reduction in sediments of the Amazon Fan, Int. J. Earth Sci., 88, 641–654, 2000.

Adler, M., Hensen, C., Wenzhöfer, F., Pfeifer, K., and Schulz, H. D.: Modeling of calcite dissolution by oxic respiration in supralysoclinal deep-sea sediments, Mar. Geol., 177, 167–189, 2001.

Aller, R. C.: Quantifying solute distributions in the bioturbated zone of marine sediments by defining an average microenvironment, Geochim. Cosmochim. Ac., 44, 1955–1965, 1980.

Aller, R. C.: The importance of relict burrow structures and burrow irrigation in controlling sedimentary solute distributions, Geochim. Cosmochim. Ac., 48, 1929–1934, 1984.

Aller, R. C. and Aller, J. Y.: The effect of biogenic irrigation intensity and solute exchange on diagenetic reaction rates in marine sediments, J. Mar. Res., 56, 905–936, 1998.

Arp, A. J., Childress, J. J., and Fisher Jr., C. R.: Metabolic and blood gas transport characteristics of the hydrothermal vent bivalve calyptogena magnifica, Physiol. Zool., 57, 648–662, 1984.

Arvidson, R. S., Morse, J. W., and Joye, S. B.: The sulfur biogeochemistry of chemosynthetic cold seep communities, Gulf of Mexico, USA, Mar. Chem., 87, 97–119, 2004.

Barry, J. P., Kochevar, R. E., and Baxter, C. H.: The influence of pore-water chemistry and physiology on the distribution of vesicomyid clams at cold seeps in Monterey Bay: Implications for patterns of chemosynthetic community organization, Limnol. Oceanogr., 42, 318–328, 1997.

Berner, R. A.: Sedimentary pyrite formation, Am. J. Sci., 268, 1–23, 1970.

Boetius, A., Ravenschlag, K., Schubert, C. J., Rickert, D., Widdel, F., Gieseke, A., Amann, R., Jørgensen, B. B., Witte, U., and Pfannkuche, O.: A marine microbial consortium apparently mediating anaerobic oxidation of methane, Nature, 407, 623–626, 2000.

Bohrmann, G., Bahr, A., Brinkmann, F., Brüning, M., Buhmann, S., Diekamp, V., Enneking, K., Fischer, D., Gassner, A., von Halem, G., Huettich, D., Kasten, S., Klapp, S., Nasir, M., Nowald, N., Ochsenhirt, W.-T., Pape, T., Ratmeyer, V., Rehage, R., Rethemeyer, J., Reuter, M., Rossel, P., Saleem, M., Schmidt, W., Seiter, C., Stephan, S., Thomanek, K., Wittenberg, N., Yoshinaga, M., and Zonneveld, K.: Report and preliminary results of R/V Meteor cruise M74/3, Fujairah-Male, 30 October–28 November, 2007. Cold seeps of the Makran subduction zone (Continental margin off Pakistan), Berichte, Fachbereich 5, Universität Bremen,

BGD
8, 9763–9811, 2011

edited by: Bohrmann, G. and Ohling, G., Bremen, 161 pp., 2008.
Borowski, W. S., Paull, C. K., and Ussler III, W.: Marine pore-water sulfate profiles indicate in situ methane flux from underlying gas hydrate, Geology, 24, 655–658, 1996.
Boudreau, B. P.: Diagenetic models and their implementations, Springer-Verlag, New York, 1997.
Brand, T. D. and Griffiths, C.: Seasonality in the hydrography and biogeochemistry across the Pakistan margin of the NE Arabian Sea, Deep-Sea Res. Part II, 56, 283–295, 2009.
Brüchert, V.: Early diagenesis of sulfur in estuarine sediments: the role of sedimentary humic and fulvic acids, Geochim. Cosmochim. Ac., 62, 1567–1586, 1998.
Claypool, G. E. and Kaplan, I. R.: The origin and distribution of methane in marine sediments, in: Natural gases in marine sediments, edited by: Kaplan, I. R., Plenum Publishing Corporation, New York, 1974.
Cline, J. D.: Spectrophotometric determination of hydrogen sulfide in natural waters, Limnol. Oceanogr., 14, 454–458, 1969.
Dale, A. W., Sommer, S., Haeckel, M., Wallmann, K., Linke, P., Wegener, G., and Pfannkuche, O.: Pathways and regulation of carbon, sulfur and energy transfer in marine sediments overlying methane gas hydrates on the Opouawe Bank (New Zealand), Geochim. Cosmochim. Ac., 74, 5763–5784, 2010.
Dando, P. R. and Hovland, M.: Environmental effects of submarine seeping natural gas, Cont. Shelf Res., 12, 1197–1207, 1992.
de Beer, D., Sauter, E., Niemann, H., Kaul, N., Foucher, J.-P., Witte, U., Schlüter, M., and Boetius, A.: In situ fluxes and zonation of microbial activity in surface sediments of the Håkon Mosby Mud Volcano, Limnol. Oceanogr., 51, 1315–1331, 2006.
Ding, F., Spiess, V., Fekete, N., Murton, B., Brüning, M., and Bohrmann, G.: Interaction between accretionary thrust faulting and slope sedimentation at the frontal Makran accretionary prism and its implications for hydrocarbon fluid seepage, J. Geophys. Res., 115, B08106, doi:10.1029/2008JB006246, 2010.
Faber, E., Gerling, P., Berner, U., and Sohns, E.: Methane in ocean waters: Concentrations and carbon isotope variability at East Pacific Rise and the Arabian Sea, Environ. Monit. Assess., 31, 139–144, 1994.
Fossing, H., Gallardo, V. A., Jørgensen, B. B., Hüttel, M., Nielsen, L. P., Schulz, H., Canfield, D. E., Forster, S., Glud, R. N., Gundersen, J. K., Küver, J., Ramsing, N. B., Teske, A., Thamdrup, B., and Ulloa, O.: Concentration and transport of nitrate by the mat-forming

BGD
8, 9763–9811, 2011

sulphur bacterium *Thioploca*, Nature, 374, 713–715, 1995.
Fossing, H., Ferdelman, T. G., and Berg, P.: Sulfate reduction and methane oxidation in continental margin sediments influenced by irrigation (South-East Atlantic off Namibia), Geochim. Cosmochim. Ac., 64, 897–910, 2000.
Gilhooly III, W. P., Carney, R. S., and Macko, S. A.: Relationships between sulfide-oxidizing bacterial mats and their carbon sources in northern Gulf of Mexico cold seeps, Org. Geochem., 38, 380–393, 2007.
Grehan, A. J. and Juniper, S. K.: Clam distribution and subsurface hydrothermal processes at Chowder Hill (Middle Valley), Juan de Fuca Ridge, Mar. Ecol.-Prog. Ser., 130, 105–115, 1996.
Haeckel, M. and Wallmann, K.: Indications for convective flow induced by focussed fluid venting at bacterial mats, Geochim. Cosmochim. Ac., 72, A339–A405, 2008.
Haeckel, M., Boudreau, B. P., and Wallmann, K.: Bubble-induced porewater mixing: A 3-D model for deep porewater irrigation, Geochim. Cosmochim. Ac., 71, 5135–5154, 2007.
Haese, R. R.: Macrobenthic activity and its effects on biogeochemical reactions and fluxes, in: Ocean Margin Systems, edited by: Wefer, G., Billet, D., Hebbeln, D., Jørgensen, B. B., Schlüter, M., and Van Weering, T., Springer Verlag, Berlin, Heidelberg, 219–234, 2002.
Haese, R. R., Meile, C., Van Cappellen, P., and De Lange, G. J.: Carbon geochemistry of cold seeps: Methane fluxes and transformation in sediments from Kazan mud volcano, eastern Mediterranean Sea, Earth. Planet. Sc. Lett., 212, 361–375, 2003.
Haese, R. R., Hensen, C., and de Lange, G. J.: Pore water geochemistry of eastern Mediterranean mud volcanoes: Implications for fluid transport and fluid origin, Mar. Geol., 225, 191–208, 2006.
Han, M. W. and Suess, E.: Subduction-induced pore fluid venting and the formation of authigenic carbonates along the cascadia continental margin: Implications for the global Ca-cycle, Palaeogeogr. Palaeoclimatol., 71, 97–118, 1989.
Hensen, C., Zabel, M., Pfeifer, K., Schwenk, T., Kasten, S., Riedinger, N., Schulz, H. D., and Boetius, A.: Control of sulfate pore-water profiles by sedimentary events and the significance of anaerobic oxidation of methane for the burial of sulfur in marine sediments, Geochim. Cosmochim. Ac., 67, 2631–2647, 2003.
Hinrichs, K.-U., Hayes, J. M., Sylva, S. P., Brewer, P. G., and DeLong, E. F.: Methane-consuming archaebacteria in marine sediments, Nature, 398, 802–805, 1999.
Hoehler, T., Alperin, M. J., Albert, D. B., and Martens, C.: Field and laboratory studies of

BGD
8, 9763–9811, 2011

methane oxidation in an anoxic marine sediment: evidence for a methanogen-sulfate reducer consortium, Global Biogeochem. Cy., 8, 451–463, 1994.
Holmkvist, L., Ferdelman, T. G., and Jørgensen, B. B.: A cryptic sulfur cycle driven by iron in the methane zone of marine sediment (Aarhus Bay, Denmark), Geochim. Cosmochim. Ac., 75, 3581–3599, 2011.
Kaul, N., Rosenberger, A., and Villinger, H.: Comparison of measured and BSR-derived heat flow values, Makran accretionary prism, Pakistan., Mar. Geol., 164, 37–51, 2000.
Knab, N. J., Dale, A. W., Lettmann, K., Fossing, H., and Jørgensen, B. B.: Thermodynamic and kinetic control on anaerobic oxidation of methane in marine sediments, Geochim. Cosmochim. Ac., 72, 3746–3757, 2008.
Kopf, A. J.: Significance of mud volcanism, Rev. Geophys., 40, 1005, doi:10.1029/2000RG000093, 2002.
Kukowski, N., Schillhorn, T., Flueh, E. R., and Huhn, K.: Newly identified strike-slip plate boundary in the northeastern Arabian Sea, Geology, 28, 355–358, 2000.
Kukowski, N., Schillhorn, T., Huhn, K., von Rad, U., Husen, S., and Flueh, E. R.: Morphotectonics and mechanics of the central Makran accretionary wedge off Pakistan, Mar. Geol., 173, 1–19, 2001.
Kuznetsov, A. P. and Levenshtein, R. Y.: Pavelius uschakovi gen. et sp. n. (Polychaeta, Ampharetidae) from the area of the Paramushir gas hydrate vent in the Sea of Okhotsk, Zoologicheskiy Zhurnal, 6, 819–825, 1988 (in Russian).
Leloup, J., Loy, A., Knab, N. J., Borowski, C., Wagner, M., and Jorgensen, B. B.: Diversity and abundance of sulfate-reducing microorganisms in the sulfate and methane zones of a marine sediment, Black Sea, Environ. Microbiol., 9, 131–142, 2007.
Levin, L. A.: Ecology of cold seep sediments: interactions of fauna with flow, chemistry and microbes, Oceanogr. Mar. Biol., 43, 1–46, 2005.
Levin, L., Ziebis, W., Mendoza, G. F., Growney, V. A., Tryon, M., Brown, K. M., Mahn, C., Gieskes, J. M., and Rathburn, A. E.: Spatial heterogeneity of macrofauna at northern California methane seeps: influence of sulfide concentration and fluid flow, Mar. Ecol.-Prog. Ser., 265, 123–139, 2003.
Lichtschlag, A., Felden, J., Brüchert, V., Boetius, A., and de Beer, D.: Geochemical processes and chemosynthetic primary production in different thiotrophic mats of the Håkon Mosby Mud Volcano (Barents Sea), Limnol. Oceanogr., 55, 931–949, 2010a.
Lichtschlag, A., Felden, J., Wenzhöfer, F., Schubotz, F., Ertefai, T. F., Boetius, A., and de Beer,

BGD
8, 9763–9811, 2011

D.: Methane and sulfide fluxes in permanent anoxia: In situ studies at the Dvurechenskii mud volcano (Sorokin Trough, Black Sea), Geochim. Cosmochim. Ac., 74, 5002–5018, 2010b.
Linke, P., Suess, E., Torres, M., Martens, V., Rugh, W. D., Ziebis, W., and Kulm, L. D.: In situ measurement of fluid flow from cold seeps at active continental margins, Deep-Sea Res. Pt. I, 41, 721–739, 1994.
Linke, P., Wallmann, K., Suess, E., Hensen, C., and Rehder, G.: In situ benthic fluxes from an intermittently active mud volcano at the Costa Rica convergent margin, Earth. Planet. Sc. Lett., 235, 79–95, 2005.
Luff, R. and Wallmann, K.: Fluid flow, methane fluxes, carbonate precipitation and biogeochemical turnover in gas hydrate-bearing sediments at Hydrate Ridge, Cascadia Margin: numerical modeling and mass balances, Geochim. Cosmochim. Ac., 67, 3403–3421, 2003.
Meile, C., Koretsky, C., and van Cappellen, P.: Quantifying bioirrigation in aquatic sediments: an inverse modeling approach., Limnol. Oceanogr., 46, 164–177, 2001.
Nelson, D. C., Jorgensen, B. B., and Revsbech, N. P.: Growth pattern and yield of a chemoautotrophic Beggiatoa sp. in oxygen-sulfide microgradients, Appl. Environ. Microbiol., 52, 225–233, 1986.
Niemann, H., Lösekann, T., de Beer, D., Elvert, M., Nadalig, T., Knittel, K., Amann, R., Sauter, E. J., Schlüter, M., Klages, M., Foucher, J. P., and Boetius, A.: Novel microbial communities of the Haakon Mosby mud volcano and their role as a methane sink, Nature, 443, 854–858, 2006.
Niemann, H., Fischer, D., Graffe, D., Knittel, K., Montiel, A., Heilmayer, O., Nöthen, K., Pape, T., Kasten, S., Bohrmann, G., Boetius, A., and Gutt, J.: Biogeochemistry of a low-activity cold seep in the Larsen B area, western Weddell Sea, Antarctica, Biogeosciences, 6, 2383–2395, doi:10.5194/bg-6-2383-2009, 2009.
Nikolovska, A., Sahling, H., and Bohrmann, G.: Hydroacoustic methodology for detection, localization, and quantification of gas bubbles rising from the seafloor at gas seeps from the eastern Black Sea, Geochem. Geophy. Geosy., 9, Q10010, doi:10.1029/2008GC002118, 2008.
O'Hara, S. C. M., Dando, P. R., Schuster, U., Bennis, A., Boyle, J. D., Chui, F. T. W., Hatherell, T. V. J., Niven, S. J., and Taylor, L. J.: Gas seep induced interstitial water circulation: observations and environmental implications, Cont. Shelf Res., 15, 931–948, 1995.
Olson, D. B., Hitchcock, G. L., Fine, R. A., and Warren, B. A.: Maintenance of the low-oxygen layer in the central Arabian Sea, Deep-Sea Res. Pt II, 40, 673–685, 1993.

BGD
8, 9763–9811, 2011

Pfeifer, K., Hensen, C., Adler, M., Wenzhöfer, F., Weber, B., and Schulz, H. D.: Modeling of subsurface calcite dissolution, including the respiration and reoxidation processes of marine sediments in the region of equatorial upwelling off Gabon, Geochim. Cosmochim. Ac., 66, 4247–4259, 2002.

Reitz, A., Pape, T., Haeckel, M., Schmidt, M., Berner, U., Scholz, F., Liebetrau, V., Aloisi, G., Weise, S. M., and Wallmann, K.: Sources of fluids and gases expelled at cold seeps offshore Georgia, eastern Black Sea, Geochim. Cosmochim. Ac., 75, 3250–3268, 2011.

Ritger, S., Carson, B., and Suess, E.: Methane-derived authigenic carbonates formed by subduction-induced pore-water expulsion along the Oregon/Washington margin, Geol. Soc. Am. Bull., 98, 147–156, 1987.

Robinson, C. A., Bernhard, J. M., Levin, L. A., Mendoza, G. F., and Blanks, J. K.: Surficial Hydrocarbon Seep Infauna from the Blake Ridge (Atlantic Ocean, 2150 m) and the Gulf of Mexico (690–2240 m), Mar. Ecol., 25, 313–336, 2004.

Sahling, H., Rickert, D., Lee, R. W., Linke, P., and Suess, E.: Macrofaunal community structure and sulfide flux at gas hydrate deposits from the Cascadia convergent margin, NE Pacific, Mar. Ecol.-Prog. Ser., 231, 121–138, 2002.

Sahling, H., Wallmann, K., Dählmann, A., Schmaljohann, R., and Petersen, S.: The physicochemical habitat of Sclerolinum sp. at Hook Ridge hydrothermal vent, Bransfield Strait, Antarctica, Limnol. Oceanogr., 50, 598–606, 2005.

Sahling, H., Bohrmann, G., Spiess, V., Bialas, J., Breitzke, M., Ivanov, M., Kasten, S., Krastel, S., and Schneider, R.: Pockmarks in the Northern Congo Fan area, SW Africa: Complex seafloor features shaped by fluid flow, Mar. Geol., 249, 206–225, 2008.

Salman, V., Amann, R., Girnth, A.-C., Polerecky, L., Bailey, J. V., Høgslund, S., Jessen, G., Pantoja, S., and Schulz-Vogt, H. N.: A single-cell sequencing approach to the classification of large, vacuolated sulfur bacteria, Syst. Appl. Microbiol., 34, 243–259, 2011.

Schlüter, H. U., Prexl, A., Gaedicke, C., Roeser, H., Reichert, C., Meyer, H., and von Daniels, C.: The Makran accretionary wedge: sediment thicknesses and ages and the origin of mud volcanoes, Mar. Geol., 185, 219–232, 2002.

Schmaljohann, R., Drews, M., Walter, S., Linke, P., von Rad, U., and Imhoff, J. F.: Oxygen-minimum zone sediments in the northeastern Arabian Sea off Pakistan: a habitat for the bacterium Thioploca, Mar. Ecol.-Prog. Ser., 211, 27–42, 2001.

Schulz, H. N. and Jørgensen, B. B.: Big Bacteria, Annu. Rev. Microbiol., 55, 105–137, 2001.

Schulz, H. N., Jørgensen, B. B., Fossing, H., and Ramsing, N.: Community Structure of Fil-

BGD

8, 9763–9811, 2011

amentous, Sheath-Building Sulfur Bacteria, Thioploca spp., off the Coast of Chile, Appl. Environ. Microbiol., 62, 1855–1862, 1996.
Seeberg-Elverfeld, J., Schlüter, M., Feseker, T., and Kölling, M.: Rhizon sampling of porewaters near the sediment-water interface of aquatic systems, Limnol. Oceanogr.-Meth., 3, 361–371, 2005.
Sibuet, M. and Olu, K.: Biogeography, biodiversity and fluid dependence of deep-sea cold-seep communities at active and passive margins, Deep-Sea Res. Pt. II, 45, 517–567, 1998.
Sommer, S., Linke, P., Pfannkuche, O., Bowden, D. A., Haeckel, M., Greinert, J., and Thurber, A. R.: Novel cold Seep Habitat along the Hikurangi Margin (New Zealand), Geophys. Res. Abstract, 10, EGU2008-A-02387, 2008.
Sommer, S., Linke, P., Pfannkuche, O., Niemann, H., and Treude, T.: Benthic respiration in a seep habitat dominated by dense beds of ampharetid polychaetes at the Hikurangi Margin (New Zealand), Mar. Geol., 272, 223–232, 2010.
Suess, E., Bohrmann, G., von Huene, R., Linke, P., Wallmann, K., Lammers, S., Sahling, H., Winckler, G., Lutz, R. A., and Orange, D.: Fluid venting in the eastern Aleutian subduction zone, J. Geophys. Res., 103, 2597–2614, 1998.
Teske, A. and Nelson, D.: The Genera Beggiatoa and Thioploca, in: The Prokaryotes,edited by: Dworkin, M., Stanley, F., Rosenberg, E., Schleifer, K.-H., and Stackebrand, E., 784–810, Springer, Berlin, 2006.
Tishchenko, P., Hensen, C., Wallmann, K., and Wong, C. S.: Calculation of the stability and solubility of methane hydrate in seawater, Chem. Geol., 219, 37–52, 2005.
Torres, M. E., McManus, J., Hammond, D. E., de Angelis, M. A., Heeschen, K. U., Colbert, S. L., Tryon, M. D., Brown, K. M., and Suess, E.: Fluid and chemical fluxes in and out of sediments hosting methane hydrate deposits on Hydrate Ridge, OR, I: Hydrological provinces, Earth. Planet. Sc. Lett., 201, 525–540, 2002.
Tryon, M. D., Brown, K. M., Torres, M. E., Trehu, A. M., McManus, J., and Collier, R. W.: Measurements of transience and downward fluid flow near episodic methane gas vents, Hydrate Ridge, Cascadia, Geology, 27, 1075–1078, 1999.
Tryon, M. D., Brown, K. M., and Torres, M. E.: Fluid and chemical flux in and out of sediments hosting methane hydrate deposits on Hydrate Ridge, OR, II: Hydrological processes, Earth. Planet. Sc. Lett., 201, 541–557, 2002.
van Dover, C. L., Aharon, P., Bernhard, J. M., Caylor, E., Doerries, M., Flickinger, W., Gilhooly, W., Goffredi, S. K., Knick, K. E., Macko, S. A., Rapoport, S., Raulfs, E. C., Ruppel, C.,

BGD
8, 9763–9811, 2011

Salerno, J. L., Seitz, R. D., Sen Gupta, B. K., Shank, T., Turnipseed, M., and Vrijenhoek, R.: Blake Ridge methane seeps: characterization of a soft-sediment, chemosynthetically based ecosystem, Deep-Sea Res. Pt. I, 50, 281–300, 2003.

von Rad, U., Schulz, H., Khan, A. A., Ansari, M., Berner, U., Cepek, P., Cowie, G., Dietrich, P., Erlenkeuser, H., Geyh, M., Jennerjahn, T., Lückge, A., Marchig, V., Riech, V., Rösch, H., Schäfer, P., Schulte, S., Sirocko, F., Tahir, M., and Weiss, W.: Sampling the oxygen minimum zone off Pakistan: glacial-interglacial variations of anoxia and productivity (preliminary results, Sonne 90 cruise), Mar. Geol., 125, 7–19, 1995.

von Rad, U., Rösch, H., Berner, U., Geyh, M., Marchig, V., and Schulz, H.: Authigenic carbonates derived from oxidized methane vented from the Makran accretionary prism off Pakistan, Mar. Geol., 136, 55–77, 1996.

von Rad, U., Berner, U., Delisle, G., Doose-Rolinski, H., Fechner, N., Linke, P., Lückge, A., Roeser, H. A., Schmaljohann, R., Wiedicke, M., Parties, S. S., Parties, S. S., Block, M., Damm, V., Erbacher, J., Fritsch, J., Harazim, B., Poggenburg, J., Scheeder, G., Schreckenberger, B., von Mirbach, N., Drews, M., Walter, S., Ali Khan, A., Inam, A., Tahir, M., Tabrez, A. R., Cheema, A. H., Pervaz, M., and Ashraf, M.: Gas and fluid venting at the Makran accretionary wedge off Pakistan, Geo.-Mar. Lett., 20, 10–19, 2000.

Wallace, P. J., Dickens, G. R., Paull, C. K., and Ussler, W.: Effects of core retrieval and degassing on the carbon isotope composition of methane in gas hydrate and free-gas bearing sediments from the Blake Ridge, Proceedings of the Ocean Drilling Program, Scientific Results, 164, 101–112, 2000.

Wallmann, K., Linke, P., Suess, E., Bohrmann, G., Sahling, H., Schlüter, M., Dählmann, A., Lammers, S., Greinert, J., and von Mirbach, N.: Quantifying fluid flow, solute mixing, and biogeochemical turnover at cold vents of the eastern Aleutian subduction zone, Geochim. Cosmochim. Ac., 61, 5209–5219, 1997.

Wallmann, K., Drews, M., Aloisi, G., and Bohrmann, G.: Methane discharge into the Black Sea and the global ocean via fluid flow through submarine mud volcanoes, Earth. Planet. Sc. Lett., 248, 545–560, 2006.

Wenzhöfer, F., Adler, M., Kohls, O., Hensen, C., Strotmann, B., Boehme, S., and Schulz, H. D.: Calcite dissolution driven by benthic mineralization in the deep-sea: in situ measurements of Ca^{2+}, pH, pCO_2 and O_2, Geochim. Cosmochim. Ac., 65, 2677–2690, 2001.

Wyrtki, K.: Physical oceanography of the Indian Ocean, in: The biology of the Indian Ocean. Ecological Studies, edited by: Zeitschel, B., Springer Verlag, Berlin, 18–36, 1973.

BGD
8, 9763–9811, 2011

Table 1. Station list of all examined cores.

Flare	GeoB-Station	Gear	Position	Water depth [m]	GHSZ*	Habitat, Seep community	Bottom water redox
1	12320-9	PC	24°53.634 N 63°01.404 E	551	–	Habitat 1, orange microbial mat	Core-OMZ
1	12320-4	PC	24°53.634 N 63°01.404 E	551	–	Habitat 2, white microbial mat	Core-OMZ
	12312-3	MUC	24°53.072 N 63°01.641 E	654	–	Background	Core-OMZ
15	12353-5	PC	24°48.458 N 63°59.649 E	732	–	Habitat 1, orange microbial mat	Core-OMZ
15	12353-3	PC	24°48.457 N 63°59.649 E	732	–	Habitat 2, white microbial mat	Core-OMZ
	12309-3	MUC	24°52.322 N 62°59.859 E	962	+	Background	Core-OMZ
2	12315-9	PC	24°50.753 N 63°01.439 E	1025	+	Habitat 1, white/rose microbial mat, sparse polychaetes	Lower boundary of OMZ
2	12315-4	PC	24°50.753 N 63°01.439 E	1025	+	Habitat 2, polychaetes and small clams	Lower boundary of OMZ
2	12313-6	PC	24°50.828 N 63°01.419 E	1038	+	Habitat 1, white/rose microbial mat, sparse polychaetes	Lower boundary of OMZ
2	12313-12	PC	24°50.828 N 63°01.419 E	1038	+	Habitat 2, polychaetes and small clams	Lower boundary of OMZ
2	12313-13	PC	24°50.829 N 63°01.419 E	1038	+	Habitat 3, small and large clams	Lower boundary of OMZ

* GHSZ = Gas hydrate stability zone

BGD
8, 9763–9811, 2011

Table 2. Input parameters used for pore water modeling of three cores at Flare 2.

Input parameters	
Length of modeled sediment column	50 cm
Porosity (upper to lower model boundary)	0.9–0.8
Temperature	12.3 °C
Sulfate concentrations at upper model boundary	26.3–31.6 mM (see text)
Methane concentrations at lower model boundary	85 mM (see text)
Fixed sulfide concentration at lower model boundary (only GeoB 12313-6)	14 mM

BGD
8, 9763–9811, 2011

Table 3. Fluxes of dissolved sulfide and sulfate, as well as depth of steepest sulfide gradient at all seep sites. Fluxes derived from modeled pore water profiles are marked.

	Flare 2; Habitat 1 (below core OMZ)	Flare 2; Habitat 2 (below core OMZ)	Flare 2; Habitat 3 (below core OMZ)	Flare 1, 15; Habitat 2 (within core OMZ)
Organisms	White/rose colored mat, sparse polychaetes	Polychaetes, small clams	Small and large clams	White/rose colored mat
Core ID	GeoB 12315-9 GeoB 12313-6	GeoB 12315-4 GeoB 12313-12	GeoB 12313-13	GeoB 12320-4 GeoB 12353-3
Upward sulfide flux ($mol\,m^{-2}\,yr^{-1}$)	8.0 9.2	11.0 5.7	2.8	4.9 3.3
Depth of steepest sulfide gradient	7–8 cm 3–7 cm	6–8 cm 10–13 cm	15–18 cm	2–6 cm 1–5 cm
Sulfate flux into SMTZ ($mol\,m^{-2}\,yr^{-1}$)	9.3 9 (modeled)	8.0 8.4 (modeled)	6.6 (modeled)	7.1 4.5

BGD
8, 9763–9811, 2011

Table 4. Modeled rates of advection and bioirrigation obtained for three cores at Flare 2.

	Advection rate [cm yr^{-1}]	Depth-integrated bioirrigation rate [cm yr^{-1}]; at a depth of [cm]
Habitat 1, GeoB 12313-6	11	162; 4.1–5.9
Habitat 2, GeoB 12313-12	8	280; 8.0–11.5
Habitat 3, GeoB 12313-13	<1	348; 11.8–15.7
Comparable approach using CoTReM by Haese et al. (2006)	5–30	max. 300; 8–11

BGD
8, 9763–9811, 2011

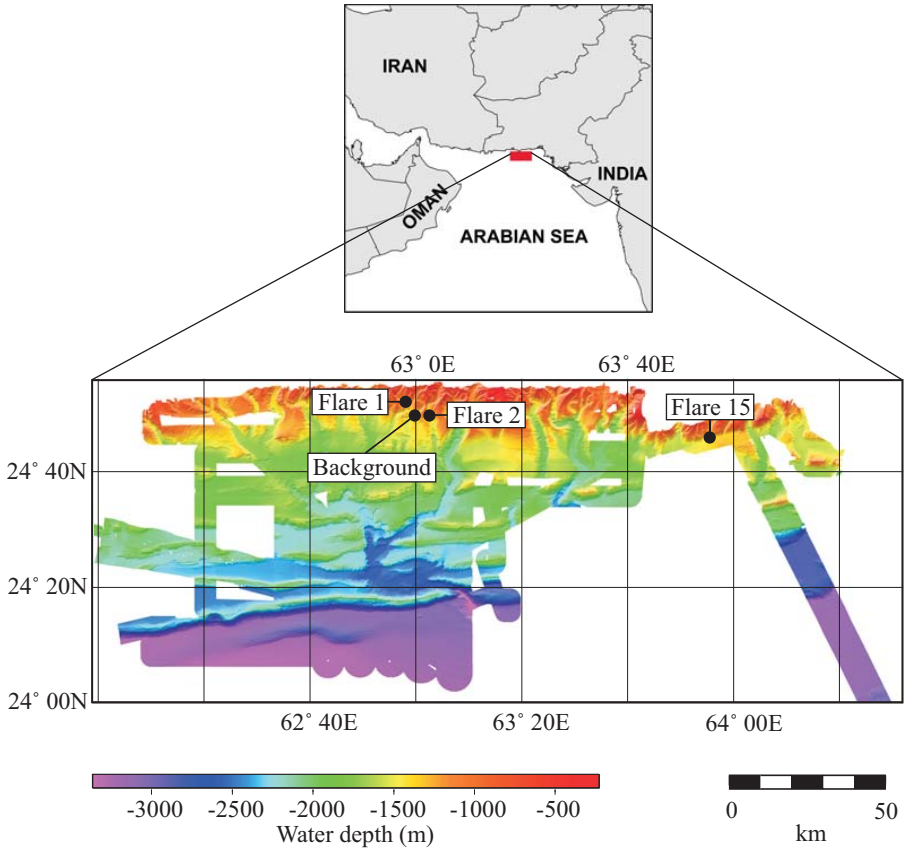

Fig. 1. Overview map of the northern Arabian Sea and detailed bathymetric map of the working area off the coast of Pakistan. Dots indicate investigated sites.

BGD
8, 9763–9811, 2011

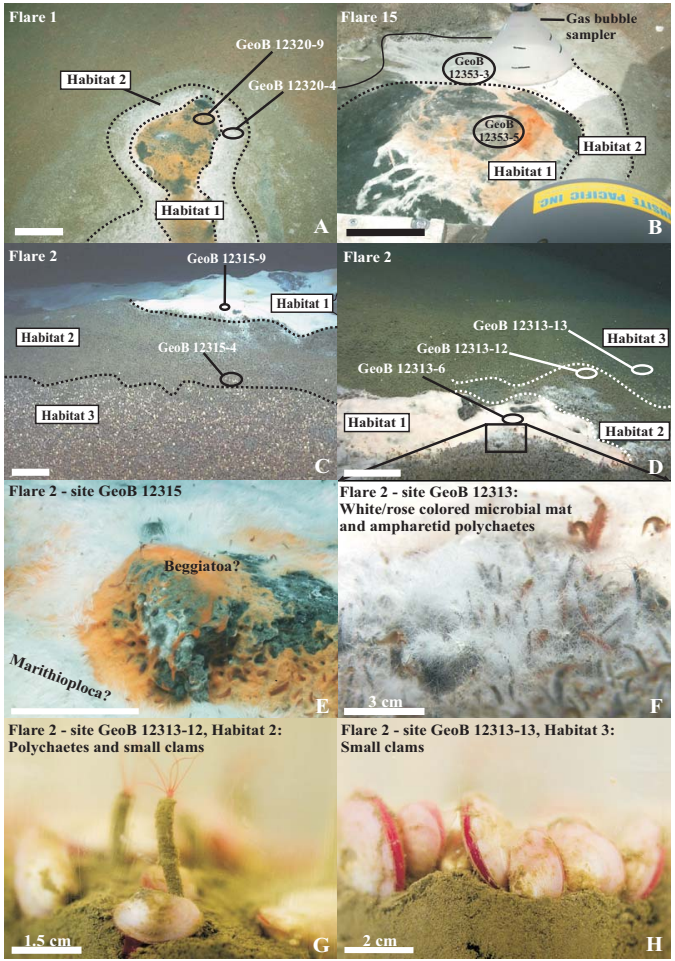

Fig. 2. Caption on next page.

BGD
8, 9763–9811, 2011

Pore water geochemistry of cold seeps offshore Pakistan

D. Fischer et al.

Fig. 2. ROV still images **(A–F)** and images of retrieved cores **(G–H)**. **(A–D)** Major habitats at all sites are encircled by stippled lines and PC positions are denoted by circles. **(E)** Close-up of Habitat 1 at site GeoB 12315, where we found microbial mats of distinctly different appearance (see text). **(F)** Close-up of the transition from Habitat 1 to Habitat 2 in **(D)**. **(G)** Appearance of Habitat 2 in the retrieved PC GeoB 12313-12. **(H)** Appearance of Habitat 3 in the retrieved PC GeoB 12313-13. Scale bar is 18 cm if not denoted otherwise.

BGD
8, 9763–9811, 2011

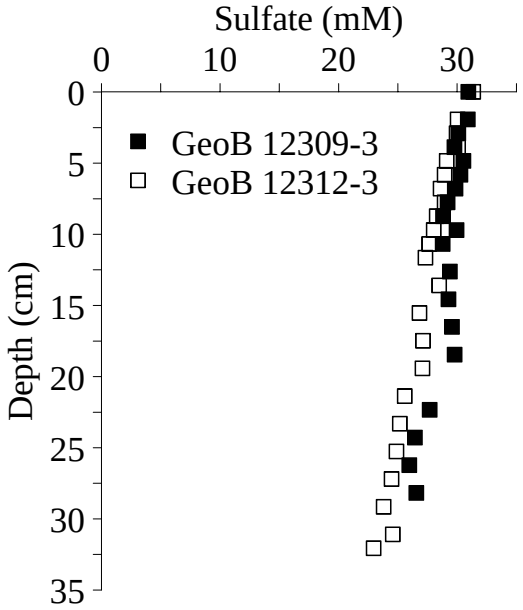

Fig. 3. Pore water sulfate profiles of non-seep reference TV-MUC cores.

BGD
8, 9763–9811, 2011

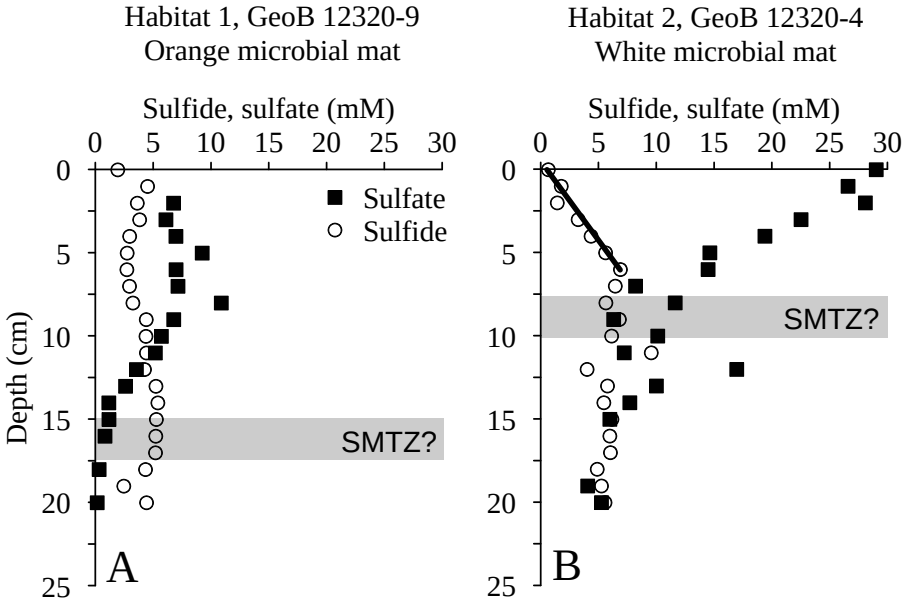

Fig. 4. Pore water profiles of sulfide and sulfate of PCs obtained for Flare 1, site GeoB 12320. The assumed depth of the SMTZ is marked by a grey box. Coring positions are marked in Fig. 2 and sampling coordinates are given in Table 1.

BGD
8, 9763–9811, 2011

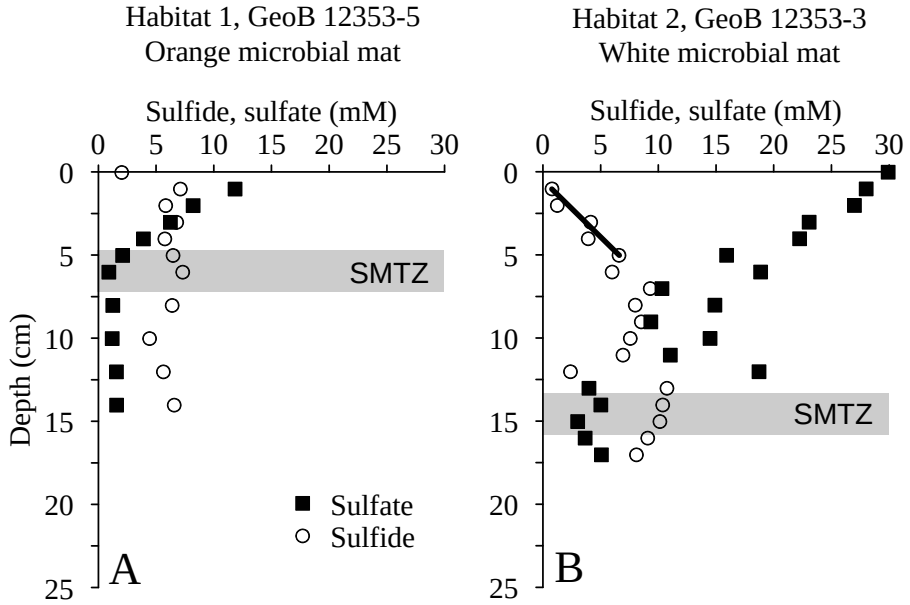

Fig. 5. Pore water profiles of sulfide and sulfate of PCs obtained for Flare 15, site GeoB 12353. See caption of Fig. 4 for further details.

BGD
8, 9763–9811, 2011

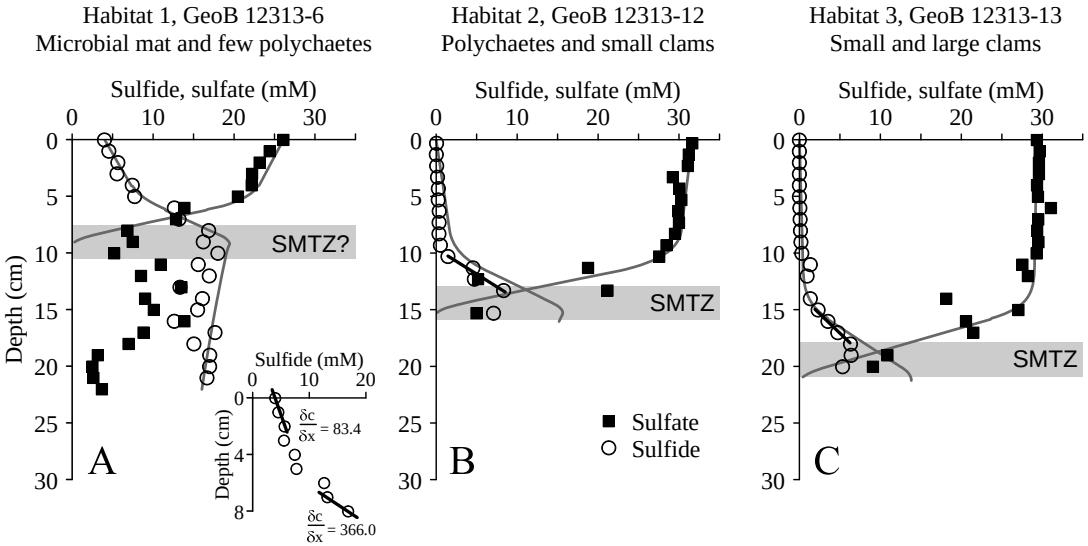

Fig. 6. Pore water profiles of measured (symbols) and modeled (lines) solutes of PCs obtained for Flare 2, site GeoB 12313. See caption of Fig. 4 for further details.

BGD
8, 9763–9811, 2011

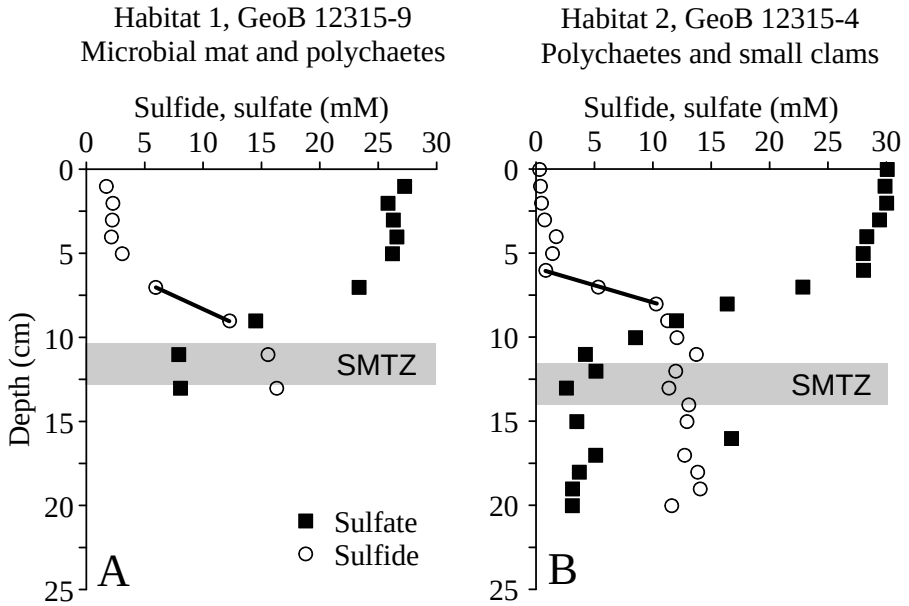

Fig. 7. Pore water profiles of sulfide and sulfate of PCs obtained for Flare 2, site GeoB 12315. See caption of Fig. 4 for further details.

BGD
8, 9763–9811, 2011

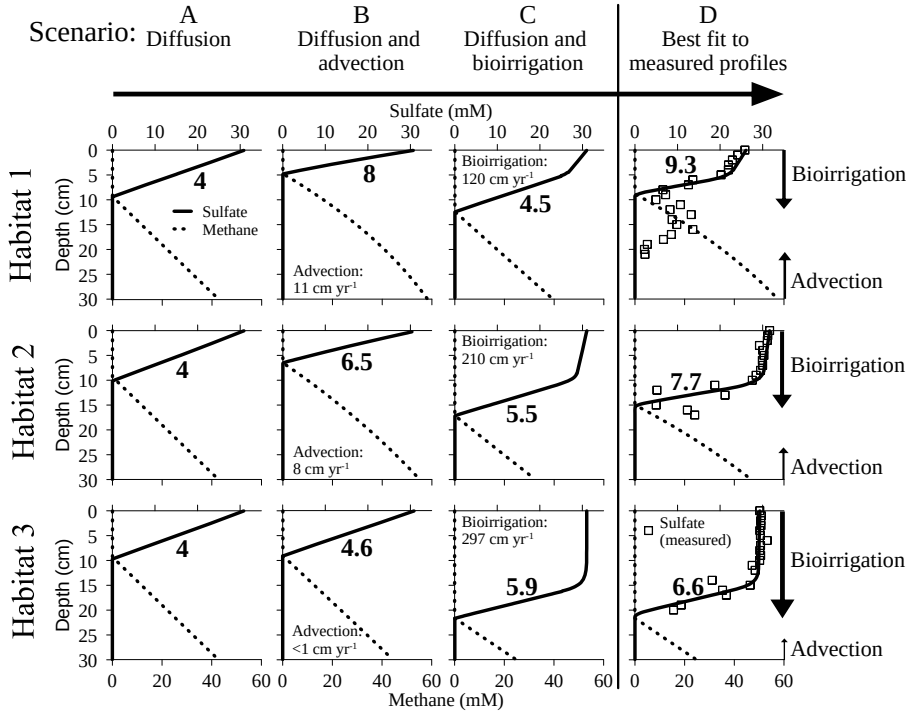

Fig. 8. Stepwise development of modeled sulfate and methane concentration profiles from a diffusively controlled system towards the observed state including advection and bioirrigation. Columns A–D indicate different "scenarios" whereas rows indicate the three different habitats at site GeoB 12313. Bold numbers next to concentration profiles depict modeled fluxes of sulfate into the SMTZ. The arrows on the right indicate the relative magnitude of the indicated transport processes.

BGD
8, 9763–9811, 2011

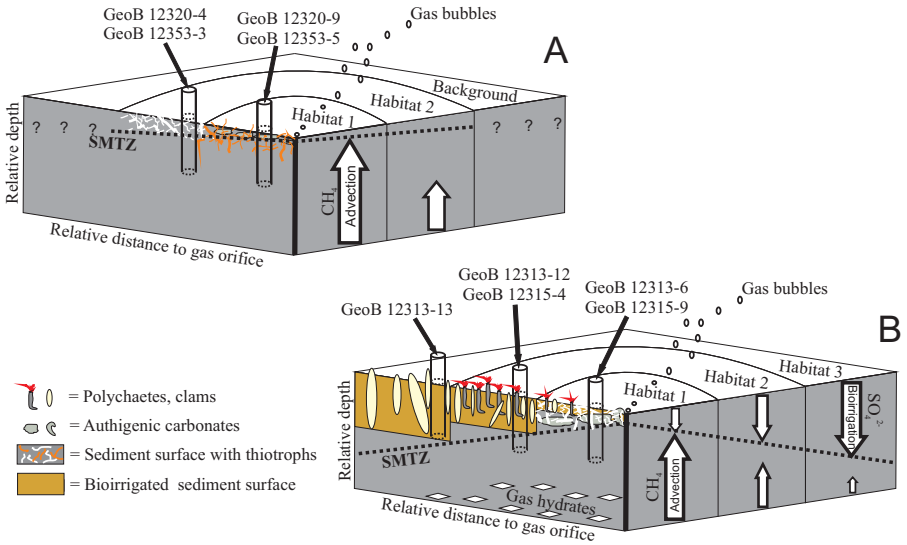

Fig. 9. Schematic illustration of the investigated seeps indicating how chemosynthetic communities determine the depth of the SMTZ. **(A)** Situation within the core-OMZ. Oxygen deficiency in the bottom water does not allow for metazoan life and thus microbial mats are the only organisms observed at Flares 1 and 15. The microbes do not irrigate the sediment surface. Advection is expected at least in Habitat 1 where bubble escape was observed and where sulfate profiles are curved concave-down. **(B)** Situation at the lower boundary of the OMZ. Slightly increased oxygen contents sustain chemosynthetic communities represented by the observed polychaetes and clams at Flare 2. Compared to the core-OMZ sites intense bioirrigation leads to a downward shift of the SMTZ due to high fluxes of sulfate into the sediment and thus compensates upward advection in all habitats.

BGD
8, 9763–9811, 2011